Eugene C. Lundquist

RESTRICTED

NATIONAL ADVISORY COMMITTEE FOR AERONAUTICS

TECHNICAL NOTE

No. 953

TORSION TEST TO FAILURE OF A MONOCOQUE BOX

By A. E. McPherson, D. Goldenberg, and G. Zibritosky
National Bureau of Standards

Washington
October 1944

RESTRICTED

NATIONAL ADVISORY COMMITTEE FOR AERONAUTICS

TECHNICAL NOTE NO. 953

TORSION TEST TO FAILURE OF A MONOCOQUE BOX

By A. E. McPherson, D. Goldenberg, and G. Zibritosky

SUMMARY

The torsion test to failure is described for a monocoque box of 24S-T aluminum alloy. The box had a rectangular section and was reinforced by Z-stringers, antirolls, bulkheads, and corner posts. The twist and strains in the stringers, sheet, corner posts, and bulkheads were measured for loads practically up to failure. Failure occurred by tearing of the cover sheet subsequent to failure of rivets joining antirolls to corner posts.

The buckling loads of the cover sheets and of the shear webs agreed with the computed values. The measured twists agreed within 6×10^{-5} radian per inch with those computed from a theory which treats the box as an assembly of four beams with wide webs, joined at the extreme fibers; the effect of buckling is taken into account in the theory by treating the web as a diagonal tension field following Wagner and Langhaar. The measured stresses in the sheet were somewhat smaller than those indicated by the theory.

The theory indicates the presence of excessive shearing stress before failure in the rivets joining the antirolls to the corner posts.

INTRODUCTION

This report describes the last one of a series of experimental studies of a monocoque box beam of representative design. Previous reports (references 1, 2, and 3) give strains, buckling loads, and deformations in the elastic range for three types of loading, compression (reference 1), cantilever bending and pure bending (reference 2), and torsion (reference 3). In

each case the measured strains and deformations were compared with theoretical values. The compression test and bending test showed substantial agreement with the predictions of classical theory. The torsion test showed large deviations from the classical (Saint-Venant) theory. It was decided to test the box to failure in torsion, in order to follow these deviations further, beyond the elastic range.

This investigation, conducted at the National Bureau of Standards, was sponsored by, and conducted with financial assistance from, the National Advisory Committee for Aeronautics.

SPECIMEN

The dimensions of the monocoque box specimen are given in figure 1. The box was fabricated from 24S-T aluminum alloy; 0.075-inch sheet was used for the shear web sides, and 0.026-inch sheet reinforced by Z-stringers, spaced 4 inches on centers, was used for the top and the bottom sides of the box. The stringers were fastened to the sheet by 1/8-inch brazier-head rivets, spaced 7/8 inch on centers. Transverse reinforcement was provided by four intermediate bulkheads and antiroll members, spaced at 19 inches.

Particular care was taken in reinforcing the ends of the box to avoid stress concentration. The reinforcements, consisting of steel angles and plates, are shown in figures 1, 2, and 3. Figure 3 also shows the construction of the bulkheads.

Tensile and compressive stress-strain curves of material from the corner posts, the stringers, and the sheet used in the monocoque box are given in reference 1. Values of Young's modulus and of yield strength (0.002-offset) obtained from the stress-strain curves are listed in table I.

TEST PROCEDURE

The specimen was mounted on a heavy steel I-beam C (figs. 4 and 5). The north end (fig. 4) was held fixed by bolting it to the I-beam. The south end (fig. 5) was mounted free to rotate about a knife edge G at the center of gravity of the section. A torque about G was applied by pulling together the lateral extension I fastened to the south end of

the specimen and the lateral extension M fastened to the I-beam C. The lateral extensions I and M were brought together by connecting them with a tensile linkage NKL which could be tightened by drawing up on the nut L. The torque was computed from the measured moment arm GN and the force in the linkage measured with the proving ring K, taking due account of the angle between GN and NL.

The twist between adjacent bulkheads was measured, as in reference 3, by the change in angle between two reflecting surfaces. The twist gages are indicated as O in figures 4, 5, and 6. The gage length was about 19 inches. The least count was about 0.5×10^{-6} radian per inch.

The strains in the specimen were measured with Tuckerman optical strain gages (used alone or with suitable adapters as described in reference 1) and with Baldwin Southwark type R-1 wire strain gage rosettes. The change in resistance of the wire strain gages was determined on a Wheatstone bridge having a strain sensitivity of 10^{-6}. The switches used in connecting different gages to the bridge were selected to have a low and constant contact resistance. The resistance-measuring apparatus is shown at P in figure 6, and one of the wire strain gage rosettes is shown at Q. One pair of rosettes was attached to the cover sheet, one pair to the shear web, and three pairs to the bulkheads.

The buckling loads of the sheet were determined by frequent visual inspection and also by the rapid divergence of the strain readings on the two sides of the sheet after buckling.

A correction of the readings of the Tuckerman gages for the effect of temperature variations was obtained from a control gage R (fig. 4) mounted on a small piece of aluminum alloy near the specimen. Temperature compensation in the case of the wire strain gages was obtained by having a wire strain gage S (fig. 6) in the balancing arm of the Wheatstone bridge.

RESULTS

The measured twists between bulkheads are shown in figure 7. The twist was measured on the diagonally opposite lower east and upper west corner posts. The twists on the lower east and upper west corner posts were nearly the same. The measured twist between bulkheads 1 and 2 and between bulkheads 3 and 4

was somewhat greater than the measured twist at the center of the box between bulkheads 2 and 3. The measured twist at the ends of the box was smaller than the other measured twists.

For moments greater than about 100,000 pound-inches the moment-twist curves of figure 7 show a decrease in slope. The average slope of the moment twist curves between bulkheads 1 and 4 dropped from 540×10^6 pound-inches per radian per inch before buckling to 370×10^6 pound-inches per radian per inch after buckling. This represents a loss in stiffness of about 32 percent.

The apparent difference in twist of the N and S ends of the box after buckling, as shown in figure 7, is probably due to the difference in location of the measuring gages rather than to any actual difference in behavior at the two ends. The gages at the S end were located in a corner toward which the diagonal-tension buckles pointed, while the gages at the N end were located in the other corners. This would indicate that near the ends of the box the diagonal tension buckles cause some parts of the cross-section to twist more than others. This effect is most marked when comparing the N-1 and 4-S locations, and, to a lesser extent, it is true in comparing the 1-2 and 3-4 locations.

The bulkheads resist warping of the box by applying shearing forces. These shearing forces may be expected to be a maximum near the ends where the resistance to warping is greatest. The measured strains on end bulkhead 1 are shown in figures 8 and 9. These strains are converted to median fiber strains in figure 10. Figure 10 indicates warping of the bulkhead such that the distance decreased between the top west corner post and the bottom east corner post.

The strain in the top east corner of bulkhead 2 is shown in figure 11. The bending and median fiber strains at this location were small.

The strain in the top cover sheet between bulkheads 1, and 2 is shown in figure 12. The difference in strain on the two faces of the top cover sheet was small up to a twisting moment of about 60,000 pound-inches. Above this moment the difference was large especially for gage line 1 which was perpendicular to the direction of the diagonal tension buckles.

The strains given in figure 12 were used to compute the maximum and minimum median fiber stresses and their directions.

The results of the computation using a Young's modulus of 10.6×10^6 psi and a Poisson's ratio of 0.32 are given in figure 13. The minimum stress increased with increasing load to a maximum value of about 5200 psi in compression at a torque of 110,000 pound-inches. At larger torques the stress decreased slowly until at 287,000 pound-inches it had a magnitude of only 2200 psi in compression. The maximum stress increased continuously with the applied moment. The rate of increase became more rapid after the sheet buckled. The angle α at which the maximum stress acted was 45° (corresponding to simple shear) at low loads. After buckling of the sheet α decreased until at 287,000 pound-inches $\alpha = 33.5^\circ$. The angle of one of the permanent diagonal tension buckles left in the box after the maximum load of 385,000 pound-inches was 29°. No computation of stress from the strain data was made for torques higher than 287,000 pound-inches since for greater torques the material was no longer elastic and the usual method of analyzing rosettes did not apply.

The strain in the east shear web between bulkheads 2 and 3 is shown in figure 14. The difference in strain on the two faces of the shear web was small up to a twisting moment of about 250,000 pound-inches. Above this the difference was large especially for gage line 1 which was perpendicular to the direction of the diagonal tension buckles.

Figure 15 shows maximum and minimum median fiber stresses and their direction, as computed from figure 14 with a Young's modulus of 10.6×10^6 psi and a Poisson's ratio of 0.32. Up to the twisting moment of 250,000 pound-inches corresponding to buckling of the shear web, the minimum stress increased to about 8900 psi in compression. At larger loads, the stress decreased slowly until at the maximum moment of 385,000 pound-inches it was 5500 psi in compression. The maximum stress increased continuously with the applied moment. The rate of increase became more rapid after the shear web buckled. The angle α of the maximum stress with respect to the corner post varied from 48° to 51° during the test as compared to 45° for pure shear.

Strains were measured on the middle stringers and on the corner posts using Tuckerman strain gages with suitable adapters. The results are plotted in figure 16. At a torque $T = 360,000$ pound-inches, the largest of these strains was only 0.00078 corresponding to a stress of about 8000 psi.

The buckles in the east shear web after failure of the monocoque box are shown in figure 17. There was one buckle between each bulkhead and shear web stiffener.

The buckles in the top cover sheet at failure are shown in figure 18. Buckling between both stringers and rivets was present. The buckles between rivets were especially marked where the bulkheads join the corner posts. Failure of a rivet at A and tearing of the sheet at B are shown in greater detail in figure 19.

Inspection of the box after failure showed that at many places the rivets joining the corner posts to the antirolls and bulkheads were sheared in two. The rivets joining the corner posts to the antirolls over bulkheads 2 and 3 on the top of the box were all sheared off before failure of the box. A close-up of the west end of the antiroll over bulkhead 2 is shown in figure 20. The corner post is shown to have moved sufficiently to displace permanently the bottom of the rivets about 0.1 inch past the top of the rivets.

The failure of the box was ascribed to a sequence of events somewhat as follows. With the development of the diagonal tension field the corner posts were drawn together, thereby putting increasing loads on the rivets connecting antirolls and bulkheads to corner posts. These loads led to the observed shearing-off of rivets from antirolls and bulkheads. The compressive force on the bulkheads after failure of the rivets had to be carried to the bulkhead through the thin cover sheet. This led to the severe buckling of the cover sheet at the points where the bulkheads join the corner posts.

The corner posts and the stringers were bent toward the center stringer by the diagonal tension of the cover sheet, as though they were beams supported at the bulkheads and antirolls and loaded in the plane of the sheet by the diagonal tension. The permanent set in this bending after failure measured midway between bulkheads with respect to the bulkheads, averaged 0.08 inch for the corner posts, 0.06 inch for the stringers next to the corner posts, and 0.03 inch for the stringers next to the middle stringer.

After failure the end plates of the monocoque box were removed to inspect the bulkheads. Bulkhead 1 near the north end of the box is shown in figure 21 and the bulkhead 4 near the south end of the box is shown in figure 22. Bulkhead 1 showed no sign of damage after failure; bulkhead 4 showed a permanent buckle in the top west corner near A.

ANALYSIS

An analysis of the twisting of the monocoque box before buckling is given in reference 3. The analysis is based on the assumption that the box behaves as an assembly of four beams with deep, thin webs (cover plates and shear webs) which are joined at the edges and to which transverse forces are applied at the bulkheads. The results of the analysis together with the results of computations based on Bredt's formula (reference 4) are plotted in figure 7 for comparison with the measured twist between bulkheads below the buckling torque of 58,000 inch-pounds. As was the case in the tests of reference 3, Bredt's formula is not in as good agreement with the data for loads less than the buckling loads as the analysis of reference 3, which includes the stiffening effect of corner posts and buckles.

Buckling reduced the stiffness of the box as shown in figure 7. An extensive literature has grown up around the problem of determining the effect of buckling on shearing stiffness and strength. Some of this work is described in references 5 to 12.

Wagner (reference 5) introduced the concept of a "tension field." He postulated that the additional shear load carried by a thin sheet web after buckling is chiefly carried by tension in the direction of the sheet buckles. Wagner's concept of a tension field has been applied to a variety of structures by Kuhn (reference 6), Heck and Ebner (reference 7), Lahde and Wagner (reference 8), Schapitz (reference 9), Lipp (reference 10), and Langhaar (reference 11), Kromm and Marguerre (reference 12) give an analysis based on an energy method of the behavior of plates subjected to shear beyond the buckling limit. This analysis gives information about the shape and the intensity of the buckle pattern which cannot be obtained from Wagner's simple assumption of a tension field. It does not necessarily follow, however, that the analysis gives better values of the failing load, the bending stresses in the flanges, or the compressive stress in the struts. For these, the assumptions by Kromm and Marguerre regarding the buckle shape and the edge conditions may be no better than Wagner's assumption of a tension field.

Wagner's tension field theory was used in analyzing the present box because of its adaptability and simplicity. The effective area resisting shear was determined from Wagner's theory as shown in the following and was inserted in the theory of reference 3 to give the stress distribution in the box.

WAGNER'S DIAGONAL TENSION FIELD THEORY APPLIED TO MONOCOQUE BOX

The presentation of "diagonal tension" theory given here follows that of Langhaar (reference 11) with the following exceptions. It includes the effects of longitudinal stiffeners and of Poisson's ratio and it develops an expression for the effective area of a buckled side of the box. The notation follows that of reference 3 wherever possible.

The basic assumption of the diagonal tension theory is that after buckling the principal stresses at the median surface of the sheet consist of a tension σ in the direction of the buckles and a compression the magnitude of which is the same as τ_{cr} and the direction of which is perpendicular to the buckles.

Figure 23(a) indicates the direction of the stresses acting on a portion of the side of the box, after buckling of the sheet. Figure 23(b) shows a small triangular wedge of the buckled side of the box and the stresses acting on the edges of the wedge. The equilibrium of forces on this wedge in the x-direction gives

$$\sigma_x = \sigma \cos^2 \alpha - \tau_{cr} \sin^2 \alpha \qquad (1)$$

The equilibrium of forces in the y-direction gives

$$\tau_{xy} = (\sigma + \tau_{cr}) \sin \alpha \cos \alpha \qquad (2)$$

The equilibrium of forces in the x-direction on the wedge in figure 23(c) also gives equation (2). Equilibrium of forces in the y-direction, however, gives

$$\sigma_y = \sigma \sin^2 \alpha - \tau_{cr} \cos^2 \alpha \qquad (3)$$

Solving equation (2) for σ gives

$$\sigma = -\tau_{cr} + \frac{\tau_{xy}}{\sin \alpha \cos \alpha} \qquad (4)$$

Substituting equation (4) into equations (1) and (3) gives

$$\sigma_x = \tau_{xy} \cot \alpha - \tau_{cr} \tag{5}$$

$$\sigma_y = \tau_{xy} \tan \alpha - \tau_{cr} \tag{6}$$

It is now necessary to determine the angle of inclination α of the buckle. First, determine the strain along a line joining points on the two corner posts and making an angle β with the x-axis. The original length of this line is $\frac{2a}{\sin \beta}$, where 2a is the depth of the web joining the corner posts.

After loading, the y component of the distance between the two points is

$$2a + \gamma (2a \cot \beta) - \delta_y \tag{7}$$

where γ is the angle through which the side shears and δ_y is the average contraction of the box in the y-direction due to the tension σ_y. The x component of the distance between the two points is

$$2a \cot \beta - \delta_x \cot \beta \tag{8}$$

where δ_x is the contraction of a length 2a of the box in the x-direction due to the tension σ_x. The strain along a line at an angle β with the x-axis is therefore

$$\epsilon_\beta = \frac{\sqrt{(2a+2a\gamma \cot \beta - \delta_y)^2 + (2a-\delta_x)^2 \cot^2 \beta} - \frac{2a}{\sin \beta}}{\frac{2a}{\sin \beta}} \tag{9}$$

Since δ_y, δ_x, and $2a\gamma$ are much smaller than 2a, the radical in equation (9) may be expanded and terms involving δ_x^2, δ_y^2, $(2a\gamma)^2$, and higher powers taken as zero.

Doing this gives

$$\epsilon_\beta = \gamma \sin \beta \cos \beta - \delta_y \frac{\sin^2 \beta}{2a} - \delta_x \frac{\cos^2 \beta}{2a} \quad (10)$$

The angle β_{max} corresponding to maximum ϵ_β is given by setting $d\epsilon_\beta/d\beta = 0$. This gives

$$\tan 2\beta_{max} = \frac{2a\gamma}{\delta_y - \delta_x} \quad (11)$$

The angle β_{max} for maximum strain ϵ_β is the same as the angle α for maximum stress σ or

$$\tan 2\alpha = \frac{2a\gamma}{\delta_y - \delta_x} \quad (12)$$

The term δ_y is the average amount by which the flanges approach each other. Let d be the distance between transverse stiffeners and let A_y be their area. The stiffeners shorten an amount

$$\delta_y' = 2adt\,\sigma_y/EA_y \quad (13)$$

where t is the sheet thickness. In addition, the corner posts bend in the plane of the sheet. If the corner post has a moment of inertia J and if the stress σ_y is considered to apply a uniform load $\sigma_y t$ to the corner post, the average sag of each corner post is

$$\frac{1}{2}\delta_y'' = \frac{d^4 t\,\sigma_y}{720EJ} \quad (14)$$

From equations (13) and (14)

$$\delta_y = \delta_y' + \delta_y'' = \frac{2adt\sigma_y}{EA_y} + \frac{d^4 t\,\sigma_y}{360EJ} \quad (15)$$

If a dimensionless constant is defined as

$$\lambda_y = dt \left[\frac{d^3}{720aJ} + \frac{1}{A_y} \right] \tag{16}$$

there is obtained for the average contraction in the y-direction

$$\delta_y = \frac{2a\lambda_y}{E} \sigma_y \tag{17}$$

The term δ_x is the contraction of a length 2a of the box in the x-direction. If A_x is the longitudinal stiffening area per web

$$\delta_x = 2a \frac{2at\ \sigma_x}{EA_x} \tag{18}$$

Defining a dimensionless constant

$$\lambda_x = \frac{2at}{A_x} \tag{19}$$

gives for the average contraction in the x-direction,

$$\delta_x = \frac{2a\ \lambda_x}{E} \sigma_x \tag{20}$$

Substituting (17) and (20) in (12) gives

$$\tan 2\alpha = \frac{\gamma E}{\lambda_y \sigma_y - \lambda_x \sigma_x} \tag{21}$$

From equation (10) the principal strain ϵ when $\beta = \alpha$ is

$$\epsilon = \gamma \sin \alpha \cos \alpha - \delta_y \frac{\sin^2 \alpha}{2a} - \delta_x \frac{\cos^2 \alpha}{2a} \tag{22}$$

Since the diagonal tension σ and the transverse compression τ_{cr} are the principal stresses the strain ϵ is also given by

$$\epsilon = \frac{\sigma}{E} + \mu \frac{\tau_{cr}}{E} \tag{23}$$

Combining equations (22) and (23) and substituting for δ_y and δ_x the values given in equations (17) and (20)

$$\sigma + \mu \tau_{cr} = \gamma E \sin \alpha \cos \alpha - \lambda_y \sigma_y \sin^2 \alpha - \lambda_x \sigma_x \cos^2 \alpha \tag{24}$$

If a ratio r is defined so that

$$r = \tau_{cr}/\tau_{xy} \tag{25}$$

the results obtained from equations (4), (5), and (6) are

$$\frac{\sigma}{\tau_{xy}} = - r + \frac{1}{\sin \alpha \cos \alpha} \tag{26}$$

$$\frac{\sigma_x}{\tau_{xy}} = \cot \alpha - r \tag{27}$$

$$\frac{\sigma_y}{\tau_{xy}} = \tan \alpha - r \tag{28}$$

Substituting equations (25) to (28) into equations (21) and (24) gives

$$- r + \frac{1}{\sin \alpha \cos \alpha} + \mu r = \gamma \frac{E}{\tau_{xy}} \sin \alpha \cos \alpha - \lambda_y \sin^2 \alpha (\tan \alpha - r)$$

$$- \lambda_x \cos^2 \alpha (\cot \alpha - r) \tag{29}$$

$$\frac{\gamma E}{\tau_{xy}} = \lambda_y \tan 2\alpha\,(\tan\alpha - r) - \lambda_x \tan 2\alpha\,(\cot\alpha - r) \quad (30)$$

Eliminating $\gamma E/\tau_{xy}$ between equations (29) and (30) and solving the resultant equations for r gives

$$r = \frac{4 - \lambda_y \tan^2\alpha \tan 2\alpha \sin 2\alpha + \lambda_x \cot^2\alpha \tan 2\alpha \sin 2\alpha}{2(1-\mu)\sin 2\alpha - \lambda_y \tan\alpha \tan 2\alpha \sin 2\alpha + \lambda_x \cot\alpha \tan 2\alpha \sin 2\alpha} \quad (31)$$

Equation (31) may also be written

$$r = 1 - 2c_1\left(\frac{\pi}{4} - \alpha\right) + (6 - 4c_1c_2)\left(\frac{\pi}{4} - \alpha\right)^2 + \left[-\frac{32\mu}{3c_3} + \frac{16c_2}{3} - 8c_1c_2^2\right]\left(\frac{\pi}{4} - \alpha\right)^3 + \ldots \quad (32)$$

where α is measured in radians

$$c_1 = (\lambda_y + \lambda_x + 2 + 2\mu) / (\lambda_y - \lambda_x)$$

$$c_2 = (\lambda_y + \lambda_x + 2 - 2\mu) / (\lambda_y - \lambda_x)$$

$$c_3 = \lambda_y - \lambda_x \quad (32a)$$

Equation (30) for the angle through which the side of the box shears may be written

$$\frac{\gamma E}{2(1+\mu)\tau_{xy}} = 1 - \frac{c_3}{1+\mu}(1 - c_1c_2)\left(\frac{\pi}{4} - \alpha\right) - 2\frac{c_2c_3}{1+\mu}(1 - c_1c_2)\left(\frac{\pi}{4} - \alpha\right)^2 + \ldots \quad (33)$$

A factor K for the increase in shear deformation due to buckling will be defined so that the effective area resisting shear after buckling is (2at)/K

Then

$$\frac{2at}{K}\,\frac{E}{2(1+\mu)}\left[\gamma - \frac{2(1+\mu)\,\tau_{cr}}{E}\right] = 2at\,(\tau_{xy} - \tau_{cr}) \quad (34)$$

Substituting in equation (34) the value of γ from equation (33), the value of τ_{xy} from equation (25), and the value of r from equation (32), and solving for K gives

$$K = \frac{c_1 - \frac{c_3}{2(1+\mu)}(1-c_1c_2) + \left[2\,c_1c_2 - 3 - \frac{c_2c_3}{1+\mu}(1-c_1c_2)\right]\left(\frac{\pi}{4}-\alpha\right)}{c_1 + (2\,c_1c_2 - 3)\left(\frac{\pi}{4}-\alpha\right)} \quad (35)$$

COMPARISON BETWEEN THEORY AND EXPERIMENT

The theoretical behavior of the box after buckling was computed from the theory of reference 3 after changing the shear constant k of that reference to kK to take account of buckling of the sheet in diagonal tension in accordance with the theory of the preceding section.

The load factor r and the shear deformation factor K were computed from equations (32) and (35), respectively, using the angle α as a parameter. Values of load and shear deformation computed for the same value of α may then be plotted against each other. Before computing r as a function of α from equation (32) and K as a function of α from equation (35) it was necessary to compute c_1, c_2, and c_3 from equation (32a) and λ_y and λ_x from equations (16) and (19). The 0.026-inch cover sheets buckle first. If they are denoted by the subscript t and the shear webs by the subscript h, as was done in reference 3,

$$\left.\begin{aligned} d_t &= \text{bulkhead spacing} = \frac{l}{5} = 19 \text{ inches} \\ t_t &= \text{sheet thickness} = 0.026 \text{ inch} \\ a_t &= \text{half width of cover sheet} = 12 \text{ inches} \\ J_t &= \text{moment of inertia of corner posts resisting bending in plane of sheet} = 0.17 \text{ inch}^4 \\ A_{yt} &= \text{transverse stiffening area} = 0.42 \text{ inch}^2 \\ A_{xt} &= \text{longitudinal stiffening area} = 3.68 \text{ inches}^2 \\ \mu &= \text{Poisson's ratio} = 0.32 \end{aligned}\right\} \quad (36)$$

J_t, A_{yt}, and A_{xt} were approximated as follows:

J_t as the moment of inertia of a corner post and 2 inches of shear web for bending in the plane of the cover sheet; A_{yt} as the area of the antiroll and that part of the bulkhead which is outside of the lightening holes; and A_{xt} as the area of two corner posts, one shear web, and five stringers.

Substituting these values into equations (16) and (19) gives

$$\lambda_{yt} = 3.48, \quad \lambda_{xt} = 0.17 \qquad (37)$$

and substituting these values into equation (32a) gives with $\mu = 0.32$

$$c_{1t} = 1.900, \quad c_{2t} = 1.514, \quad c_{3t} = 3.31 \qquad (38)$$

Substituting equation (38) into equation (35) gives

$$K_t = 2.24 \frac{1 + 2.32\left(\frac{\pi}{4} - \alpha\right)}{1 + 1.44\left(\frac{\pi}{4} - \alpha\right)} \qquad (39)$$

A range of values of α from $\frac{\pi}{4}$ to 0.628 radian (i.e., 45° to 36°) gives (see equation (31)) a range of values

of $r = \tau_{cr}/\tau_{xy}$ from 1 to 0.0801 and gives (see eq. 39) a range of values of K_t from 2.24 to 2.49. An intermediate value of

$$K_t = 2.38 \tag{40}$$

corresponding to $r = 0.648$ and $\alpha = 0.706$ radian will be used in the equations of reference 3 to correct for the loss of shear strength in the cover sheets after buckling.

The value of $k_t K_t$ was used in the equations of reference 3 in place of k_t. The values of force and twist were then determined from those equations. Using the symbol Δ to indicate the increase in a quantity after buckling of the cover sheet gives:

$$\left.\begin{aligned}
\Delta T &= \text{increase in torque applied to box after buckling} \\
\Delta F_t &= 0.0128\ \Delta T \text{ pound} = \text{increase in shear force applied to cover sheet at ends of box after buckling} \\
\Delta F_h &= 0.0364\ \Delta T \text{ pound} = \text{increase in shear force applied to shear web at ends of box after buckling} \\
\Delta P_{1t} &= 0.0125\ \Delta T \text{ pound} = \text{increase in shear force applied to cover sheet at first bulkhead from ends after buckling} \\
\Delta P_{1h} &= -0.0052\ \Delta T \text{ pound} = \text{increase in shear force applied to shear web at first bulkhead from ends after buckling} \\
\Delta P_{2t} &= 0.0037\ \Delta T \text{ pound} = \text{increase in shear force applied to cover sheet at second bulkhead from ends after buckling} \\
\Delta P_{2h} &= -0.0015\ \Delta T \text{ pound} = \text{increase in shear force applied to shear web at second bulkhead from ends after buckling} \\
10^6\ \Delta\theta_3 &= 0.00294\ \Delta T \text{ radian per inch} = \text{twist between center two bulkheads} \\
10^6\ \Delta\theta_2 &= 0.00260\ \Delta T \text{ radian per inch} = \text{twist between the adjoining bulkheads}
\end{aligned}\right\} \tag{41}$$

No value was determined for the twist of the box in the end bays since the diagonal tension buckles extend over a shorter length of sheet in the end bays than in the central bays. It did not seem worthwhile to extend Wagner's theory to take account of this because of the uncertainty regarding the rigidity of the end connections. The values of twist given by equation (41) are plotted in figure 7 for torques between 58,000 inch-pounds corresponding to buckling of the cover sheet as a plate with clamped edges with $\tau_{cr} = 3790$ psi (see p. 22 of reference 3), and 239,000 inch-pounds corresponding to buckling of the shear web sides of the box as plates with simply supported edges. The buckling of the shear web sides at a torque of 239,000 inch-pounds was computed from the present theory and from reference 13. The shear web consists of rectangular panels 9.5 inches long, 6.62 inches wide, and 0.075 inch thick. With $E = 10.6 \times 10^6$ psi, reference 13 (fig. 191) gives for the buckling stress,

$$\tau_{cr} = 9100 \text{ psi} \tag{42}$$

From page 20 of reference 3 the stress in the shear web before buckling of the cover sheet is 0.0329T. The torque which just buckles the cover plate is 58,000 inch-pounds. The stress in the shear web when the cover sheet buckles is therefore

$$\tau' = 0.0329(58,000) = 1910 \text{ psi} \tag{43}$$

From page 20 of reference 3, the increase in stress $\Delta\tau$ is

$$\Delta\tau = \frac{1}{2a_h h}(\Delta F_h + \Delta P_{1h} + \Delta P_{2h}) \tag{44}$$

Substituting $a_h = 5$ inch, $h = 0.075$ inch, and the values of ΔF_h, ΔP_{1h}, and ΔP_{2h} given in equation (41) gives

$$\Delta\tau = 0.0396\ \Delta T \text{ psi} \tag{45}$$

Combining equations (42), (43), and (45) and solving for the increase in torque ΔT_{cr} necessary to raise the shear stress $\tau' + \Delta\tau$ to τ_{cr} gives,

$$\left.\begin{aligned} \Delta T_{cr} &= 181,000 \text{ inch-pounds} \\ T_{cr} &= 58,000 + \Delta T_{cr} = 239,000 \text{ inch-pounds} \end{aligned}\right\} \quad (46)$$

After buckling of the shear web, a diagonal tension field is present in both the cover sheet and the shear web. For the shear web denoted by the subscript h,

$$\left.\begin{aligned} d_h &= \text{stiffener spacing} = 9.5 \text{ inches} \\ t_h &= \text{sheet thickness} = 0.075 \text{ inch} \\ a_h' &= \text{half width of } 0.075 \text{ inch sheet} \\ &= 3.312 \text{ inches for diagonal tension theory} \\ a_h &= \text{half width of side} = 5 \text{ inches for theory of reference 3.} \\ J_h &= \text{moment of inertia of corner posts resisting bending in plane of shear web} = 0.60 \text{ inch}^4 \\ A_{yh} &= \text{transverse stiffening area} = 0.145 \text{ inch}^2 \\ A_{xh} &= \text{longitudinal stiffening area} = 1.26 \text{ inches}^2 \\ \mu &= 0.32 \end{aligned}\right\} \quad (47)$$

Substituting these values into equations (16) and (19) gives

$$\lambda_{yh} = 5.35, \quad \lambda_{xh} = 0.39 \quad (48)$$

and substituting these values into equation (32a) gives with

$$\mu = 0.32$$

$$c_{1h} = 1.69, \quad c_{2h} = 1.43, \quad c_{3h} = 4.96 \quad (49)$$

Substituting equation (49) into equation (35) gives

$$K_h = 2.54 \frac{1 + 2.20\left(\frac{\pi}{4} - \alpha\right)}{1 + 1.09\left(\frac{\pi}{4} - \alpha\right)} \quad (50)$$

A range of values of α from $\frac{\pi}{4}$ to 0.698 radian (i.e., 45° to 40°) gives a range of values of K_h from 2.54 to 2.77. This range of values is so small that the intermediate value

$$K_h = 2.6 \tag{51}$$

will be used in the equation of reference 3.

The action of the unbuckled shear web is approximated on page 18 of reference 3 by taking $k_h = 1.845$. The action after buckling will be approximated by taking

$$k_h = 1.845\ K_h$$

Theoretically there should be a decrease in effective area of the cover sheet (that is, a decrease in K_t (equation (40)) after buckling of the shear web, since part of the longitudinal stiffening area is then used by the shear web. This decrease in K_t will be neglected because K_t is relatively unaffected by reduction in the longitudinal stiffening of the cover sheet.

The values of force and of twist as determined from the equations in reference 3, after replacing k_t, k_h by k_tK_t, k_hK_h, are given below in the notation of equation (41); the symbol $\Delta\Delta$ is used to indicate the increase as a quantity after buckling of the shear web sides of the box.

$$\left.\begin{aligned}
&\Delta\Delta T = \text{increase in torque applied to box after buckling of shear web at } T = 239{,}000 \text{ inch-pounds}\\
&\Delta\Delta F_t = 0.0158\ \Delta\Delta T \text{ pound}\\
&\Delta\Delta F_h = 0.0351\ \Delta\Delta T \text{ pound}\\
&\Delta\Delta P_{1t} = 0.0112\ \Delta\Delta T \text{ pound}\\
&\Delta\Delta P_{1h} = -0.0047\ \Delta\Delta T \text{ pound}\\
&\Delta\Delta P_{2t} = 0.0033\ \Delta\Delta T \text{ pound}\\
&\Delta\Delta P_{2h} = -0.0014\ \Delta\Delta T \text{ pound}\\
&10^6\ \Delta\Delta\ \theta_3 = 0.00339\ \Delta\Delta T \text{ radian per inch}\\
&10^6\ \Delta\Delta\ \theta_2 = 0.00309\ \Delta\Delta T \text{ radian per inch}
\end{aligned}\right\} \tag{52}$$

Again, no value was determined for the twist in the end bays because a full diagonal tension field could not be developed there.

A comparison of the theoretical twist according to reference 3 and according to equations (41) and (52) and the measured twist is given in figure 7. The difference between theoretical and measured twist is less than about 0.00006 radian per inch for torques less than the torque of 270,000 inch-pounds at which yielding starts. This is comparable with the difference in measured twist at two positions on the same section of the box.

The shearing stress in the cover sheet between bulkheads 1 and 2 is given by (see p. 22 of reference 3)

$$\tau_{xy} = \frac{k_t}{A_t}(F_t + P_{1t}) = \frac{2.063}{1.290}(0.02080 + 0.01582)T = 0.0586T \quad (53)$$

before buckling of the cover sheet at $T = 58{,}000$ inch-pounds. After buckling of the cover sheet

$$\Delta\tau_{xy} = \frac{k_t K_t}{A_t}(\Delta F_t + \Delta P_{1t}) = \frac{2.063 \times 2.38}{1.290}(0.0128 + 0.0125)\Delta T$$

$$= 0.0964\,\Delta T \quad (54)$$

until buckling of the shear web at $T = 239{,}000$ inch-pounds. After buckling of the shear web

$$\Delta\Delta\tau_{xy} = \frac{k_t K_t}{A_t}(\Delta\Delta F_t + \Delta\Delta P_{1t}) = \frac{2.063 \times 2.38}{1.290}(0.0158 + 0.0112)\Delta\Delta T$$

$$= 0.103\,\Delta\Delta T \quad (55)$$

The theoretical value of maximum principal stress σ in the cover sheet was determined from equation (4) using equations

(53), (54), and (55) with $\tau_{cr} = 3790$ psi and a theoretical intermediate value of $\alpha = 40.48^\circ$ after buckling as determined in connection with equation (40). The principal stresses are plotted in figure 13 for comparison with the measured maximum and minimum principal stresses. The comparison shows that equation (4) based on Wagner's tension field theory is conservative. For the maximum stress, the theory gave stresses as much as 7000 psi higher than the measured stresses.

The shearing stress in the shear web between bulkheads 2 and 3 is given on page 20 of reference 3 as

$$\tau_{xy} = 0.0329T \qquad (56)$$

before buckling of the shear web at $T = 58{,}000$ inch-pounds. Between 58,000 and 239,000 inch-pounds the increase in shear is given by equation (45). After buckling of the shear web at $T = 239{,}000$ inch-pounds the further increase in the shear stress is

$$\Delta\Delta\tau_{xy} = \frac{K_h}{2a_h h}(\Delta\Delta F_h + \Delta\Delta P_{1h} + \Delta\Delta P_{2h})$$

$$= \frac{2.6}{0.75}(0.0351 - 0.0047 - 0.0014)\Delta\Delta T = 0.100\Delta\Delta T \qquad (57)$$

The theoretical value of maximum principal stress σ in the shear web was determined from equation (4) using equations (56), (45), (57), and (42) and a theoretical median value of $\alpha = 43^\circ$ after buckling of the shear web corresponding to the median value of K_h in equation (51). The principal stresses are plotted in figure 15 for comparison with the measured stresses. In this case, as in the case of the cover sheet, the maximum tensile stress computed from the diagonal tension theory as presented in this paper was up to 7000 psi greater than the measured stress.

It appears, therefore, that the diagonal tension theory gives values for the maximum stress, soon after buckling that are on the conservative side by a considerable margin.

No attempt was made to check the experimentally determined strains in the bulkheads (see figs. 8, 9, 10, and 11)

against computed values since the strain distribution in a bulkhead having flanged circular holes is as yet unknown even for simple stress distributions on the edges. Likewise no attempt was made to check the experimentally determined strains in the reinforcements (see fig. 16) since these strains are all relatively small for torsion.

The shear load carried by the rivets attaching the antirolls to the corner post (see fig. 20) was estimated by assuming that the antiroll and bulkhead divide the diagonal tension load on the corner post in proportion to their respective effective areas. The antiroll has an area of 0.132 inch square, while that part of the bulkhead out to the circular hole together with its reinforcing stiffener has an area of 0.292 inch square. On this basis the antiroll takes 31.1 percent of the load. The shear load on the rivets is therefore

$$\text{Rivet load} = 0.311\, \sigma_{yt} t_t d_t \tag{58}$$

where the subscript t denotes the cover sheet. From equations (6) and (36):

$$\text{Rivet load} = 0.311\ (0.026)\ (19)\ (\tau_{xy} \tan \alpha - \tau_{cr})_t$$

$$= 0.154\ (\tau_{xy} \tan \alpha - \tau_{cr})_t \tag{59}$$

The shear stress between bulkheads 2 and 3 was computed from equations analogous to equations (53) to (55) for the shear stress between bulkheads 1 and 2. The angle α was again taken as 40.48° and the critical shear stress taken as $\tau_{cr} = 3790$ psi. The computation leads to a shear load on the rivets equal to zero just before buckling of the cover sheet and a shear load equal to 2630 pounds just before buckling of the shear web at $T = 239{,}000$ inch-pounds. This rivet load corresponds to a nominal shear stress on the two 1/8-inch rivets of 107,000 psi. Even after making allowance for the roughness of the estimate it is not surprising that these rivets were found sheared in two as shown in figure 20.

National Bureau of Standards,
Washington, D. C., July 3, 1944.

REFERENCES

1. Ramberg, Walter, McPherson, Albert E., and Levy, Sam: Compressive Tests of a Monocoque Box. NACA TN No. 721, 1939.

2. McPherson, Albert E., Ramberg, Walter, and Levy, Samuel: Bending Tests of a Monocoque Box. NACA TN No. 873, 1942.

3. Levy, Samuel, McPherson, Albert E., and Ramberg, Walter: Torsion Test of a Monocoque Box. NACA TN No. 872, 1942.

4. Timoshenko, S.: Theory of Elasticity. McGraw-Hill Book Co., Inc., 1st ed., 1934, p. 270.

5. Wagner, Herbert: Flat Sheet Metal Girders with Very Thin Metal Web.

   Part I — General Theories and Assumptions. NACA TM No. 604, 1931.

   Part II — Sheet Metal Girders with Spars Resistant to Bending Oblique Uprights — Stiffness. NACA TM No. 605, 1931.

   Part III — Sheet Metal Girders with Spars Resistant to Bending the Stress in Uprights — Diagonal Tension Fields. NACA TM No. 606, 1931.

6. Kuhn, Paul: Investigations of the Incompletely Developed Plane Diagonal-Tension Field. NACA Rep. No. 697, 1940.

7. Heck, O. S., and Ebner H.: Methods and Formulas for Calculating the Strength of Plate and Shell Constructions as Used in Airplane Design. NACA TM No. 785, 1936.

8. Lahde, R., and Wagner, H.: Tests for the Determination of the Stress Condition in Tension Fields, NACA TM No. 809, 1936.

9. Schapitz E.: The Twisting of Thin-Walled Stiffened Circular Cylinders. NACA TM No. 878, 1938.

10. Lipp, James E.: Shear Field Aircraft Spars. Jour. Aero. Sci., vol. 7, Nov. 1939, p. 1.

11. Langhaar, H. L.: Theoretical and Experimental Investigations of Thin-Webbed Plate-Girder Beams, A.S.M.E., Trans., vol. 65, Oct. 1943, pp. 799-802.

12. Kromm, A., and Marguerre, K.: Behavior of a Plate Strip under Shear and Compressive Stresses beyond the Buckling Limit. NACA TM No. 870, 1938.

13. Timoshenko, S.: Theory of Elastic Stability. McGraw-Hill Book Co., Inc., 1936, p. 362.

TABLE I.- MECHANICAL PROPERTIES OF MATERIAL

Sample	Young's modulus (psi)		Yield strength (psi) (offset = 0.2 percent)		Tensile strength (psi)	Elongation in 2 inches (percent)
	Tension	Compression	Tension	Compression		
Corner angle	10.4×10^6	10.8×10^6	48,000	42,000	61,600	21
Stringer 2	10.4	10.8	48,300	40,700	63,110	25
Stringer 1	10.4	10.8	48,700	40,500	63,100	25
0.075-inch shear web	10.5	10.7	53,700	44,000	70,020	20
0.026-inch top and bottom plating	10.5	10.8	57,100	46,800	73,500	18

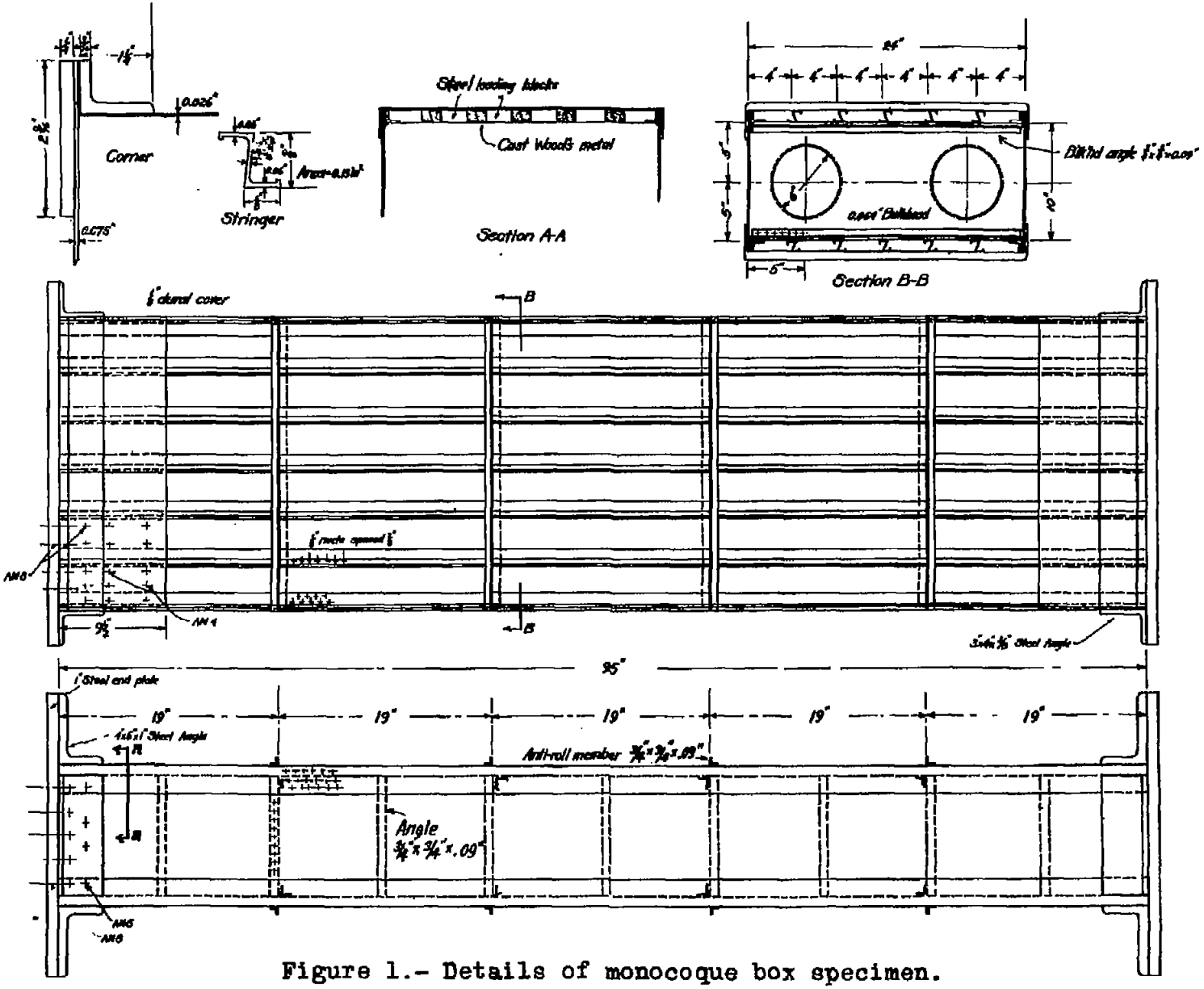

Figure 1.- Details of monocoque box specimen.

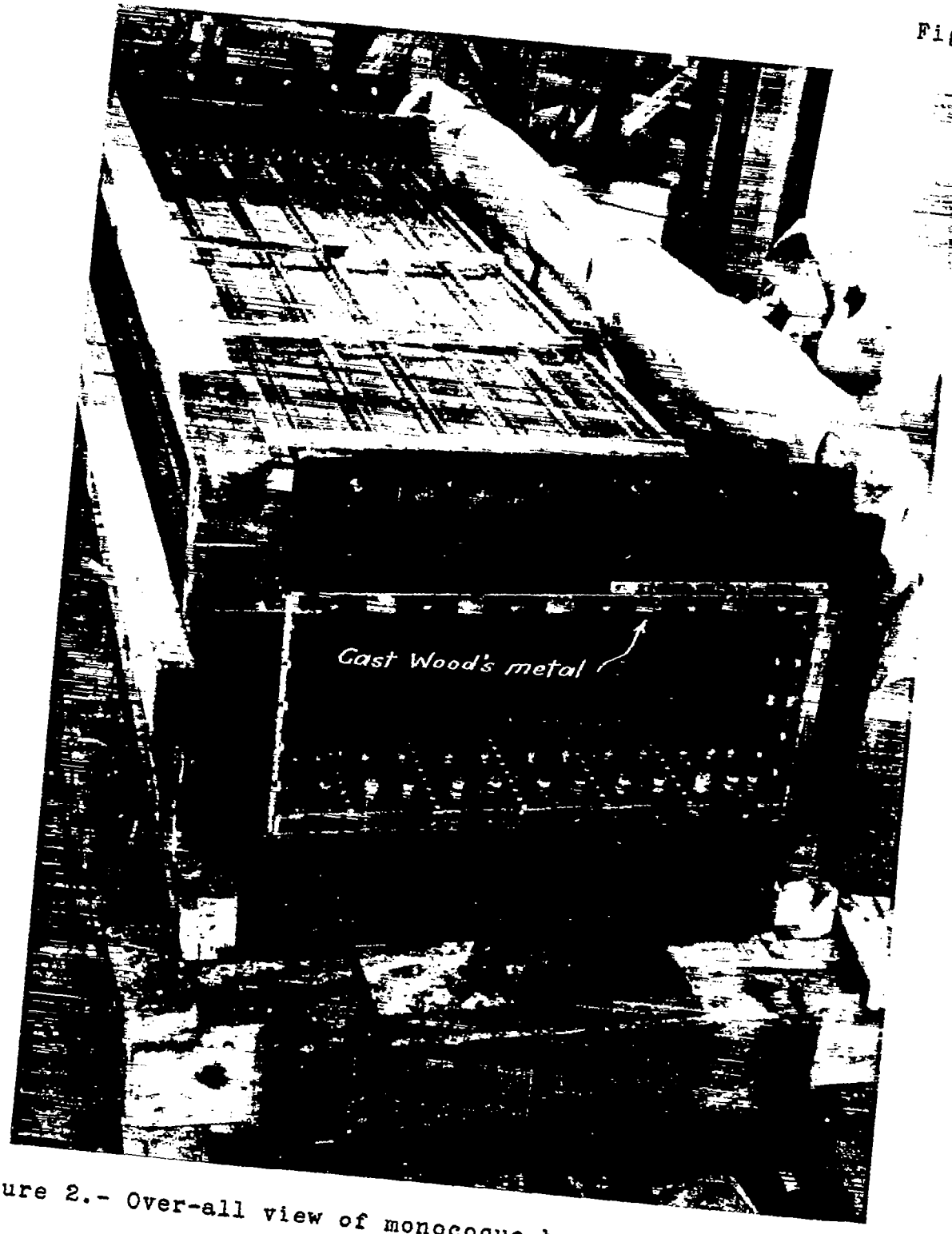

Figure 2.- Over-all view of monocoque box (end plate removed).

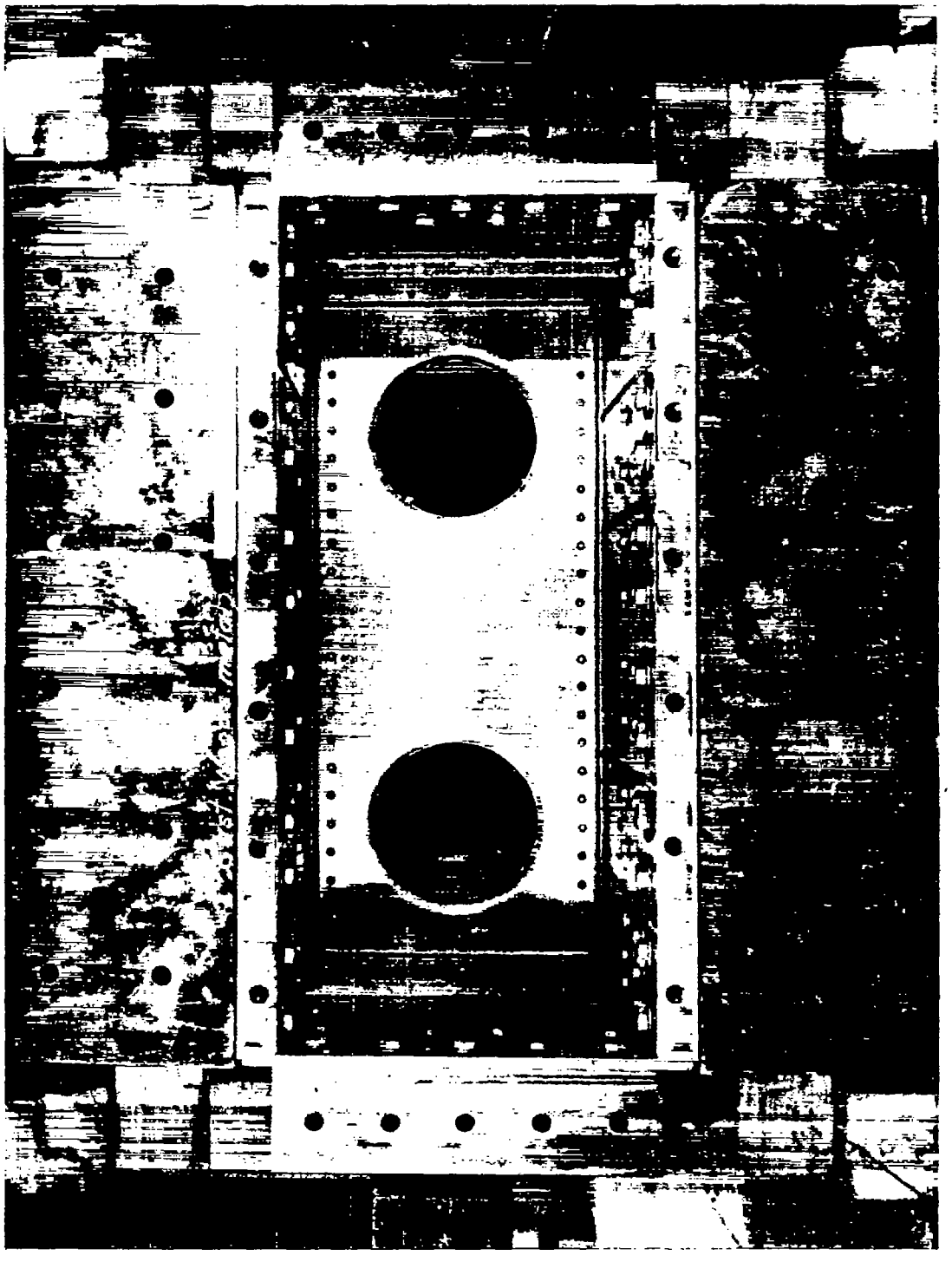

Figure 3.- End view of monocoque box (end plate removed).

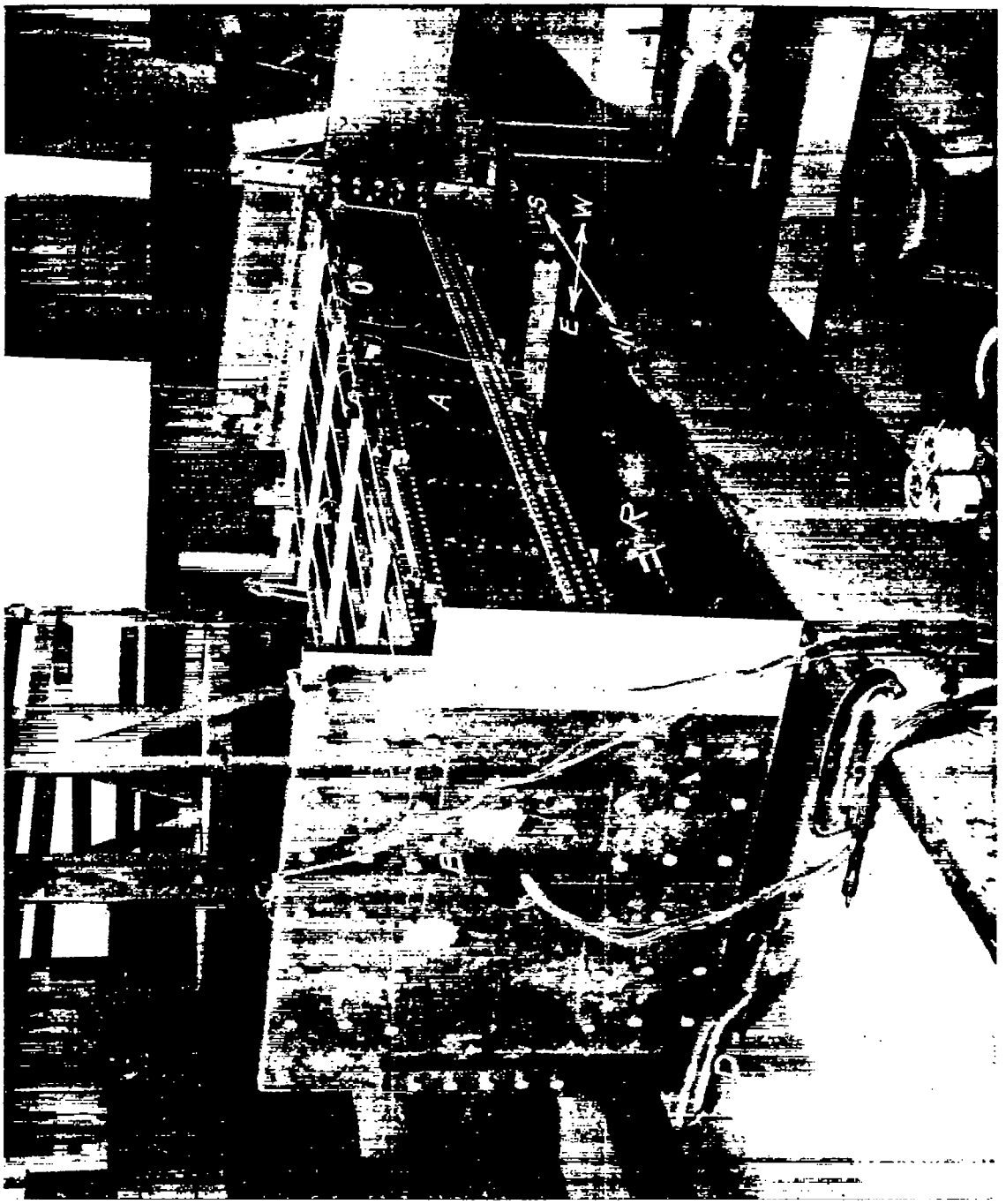

Figure 4.- Fixed end of the monocoque box specimen at a load of 220,000 lb - in.

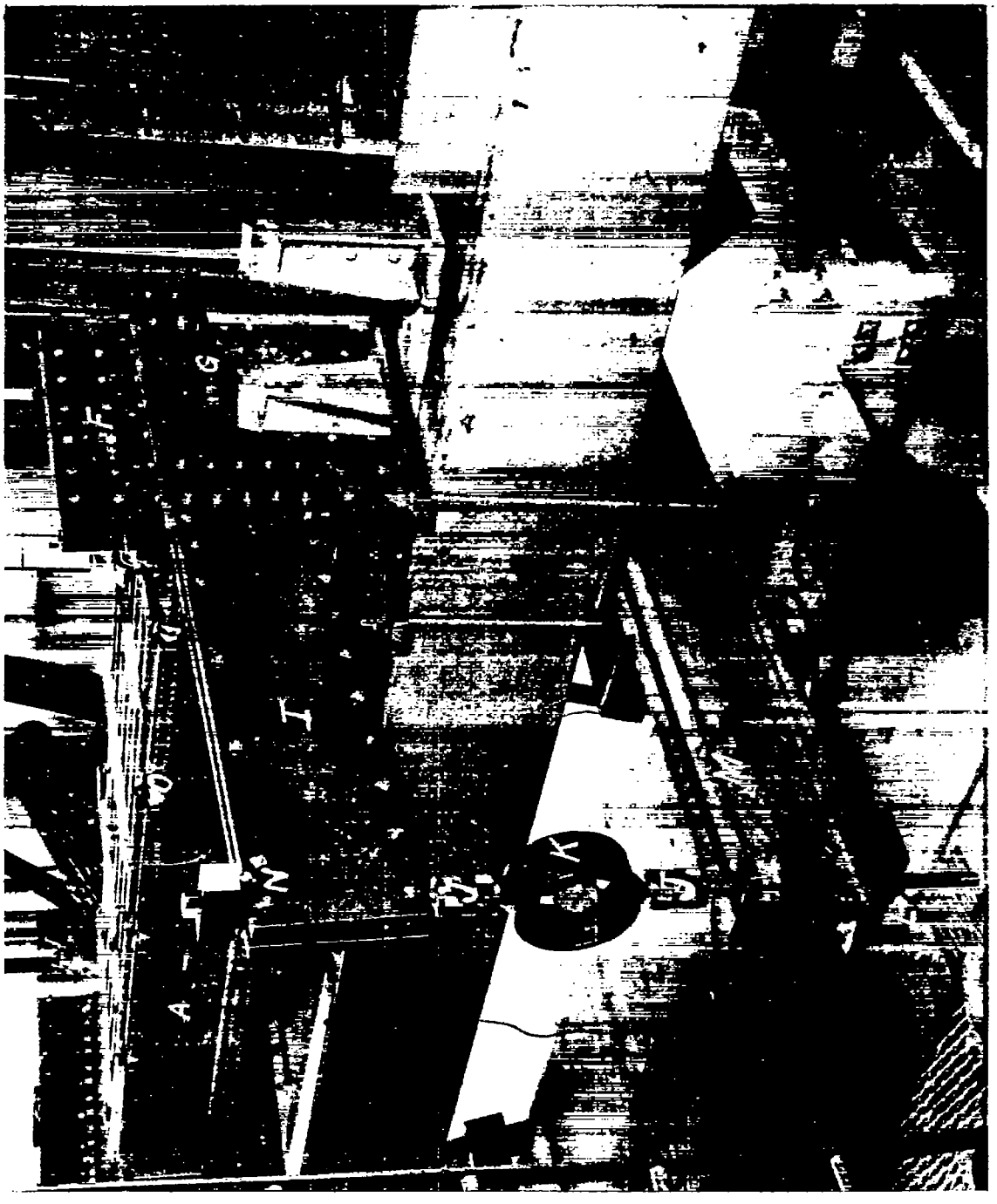

Figure 5.- Pivoted end of the monocoque box specimen at a load of 220,000 lb - in.

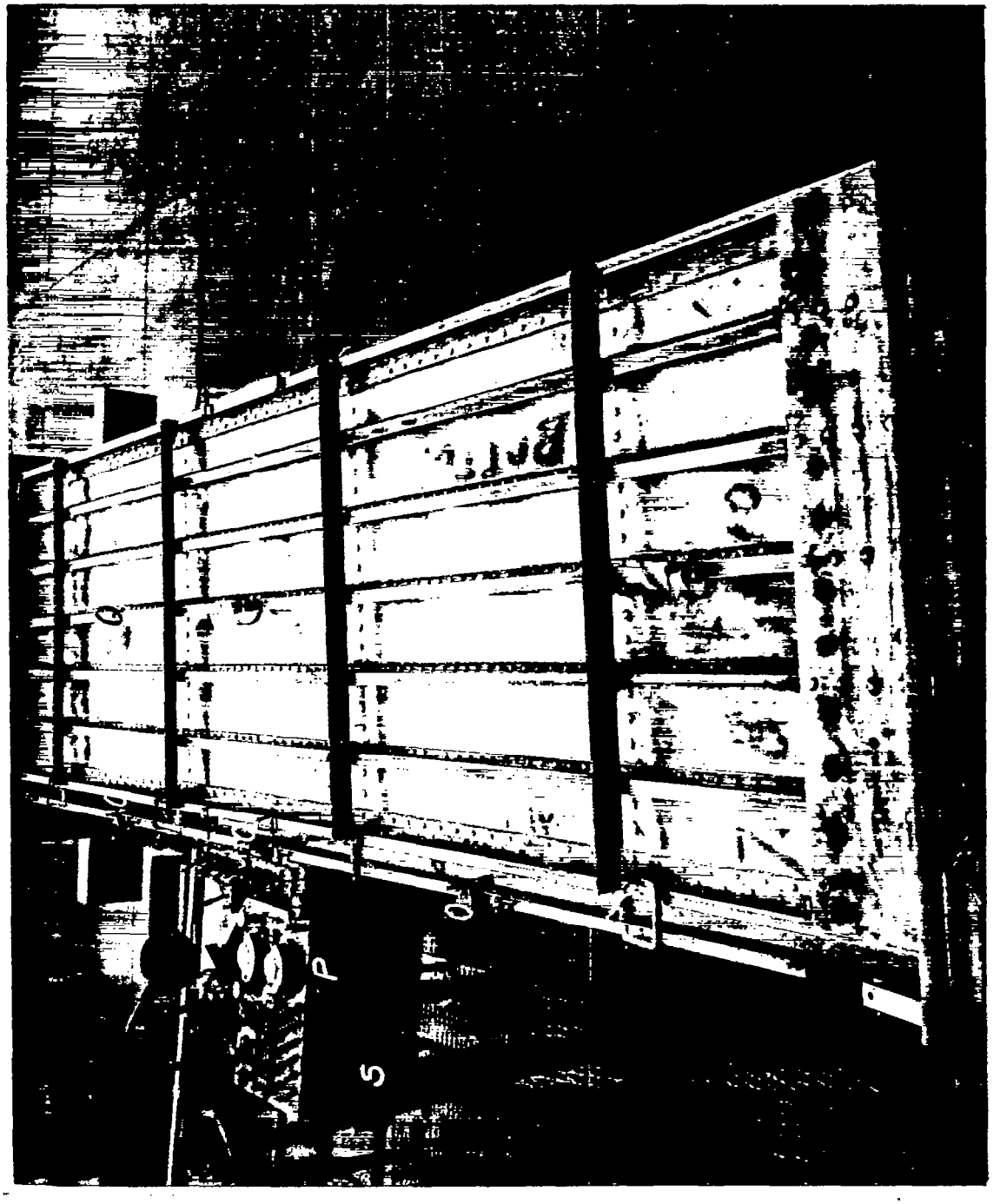

Figure 6.- Apparatus for measuring change in resistance of wire strain gages and view of cover plate of box showing shear wrinkles at 220,000 lb - in.

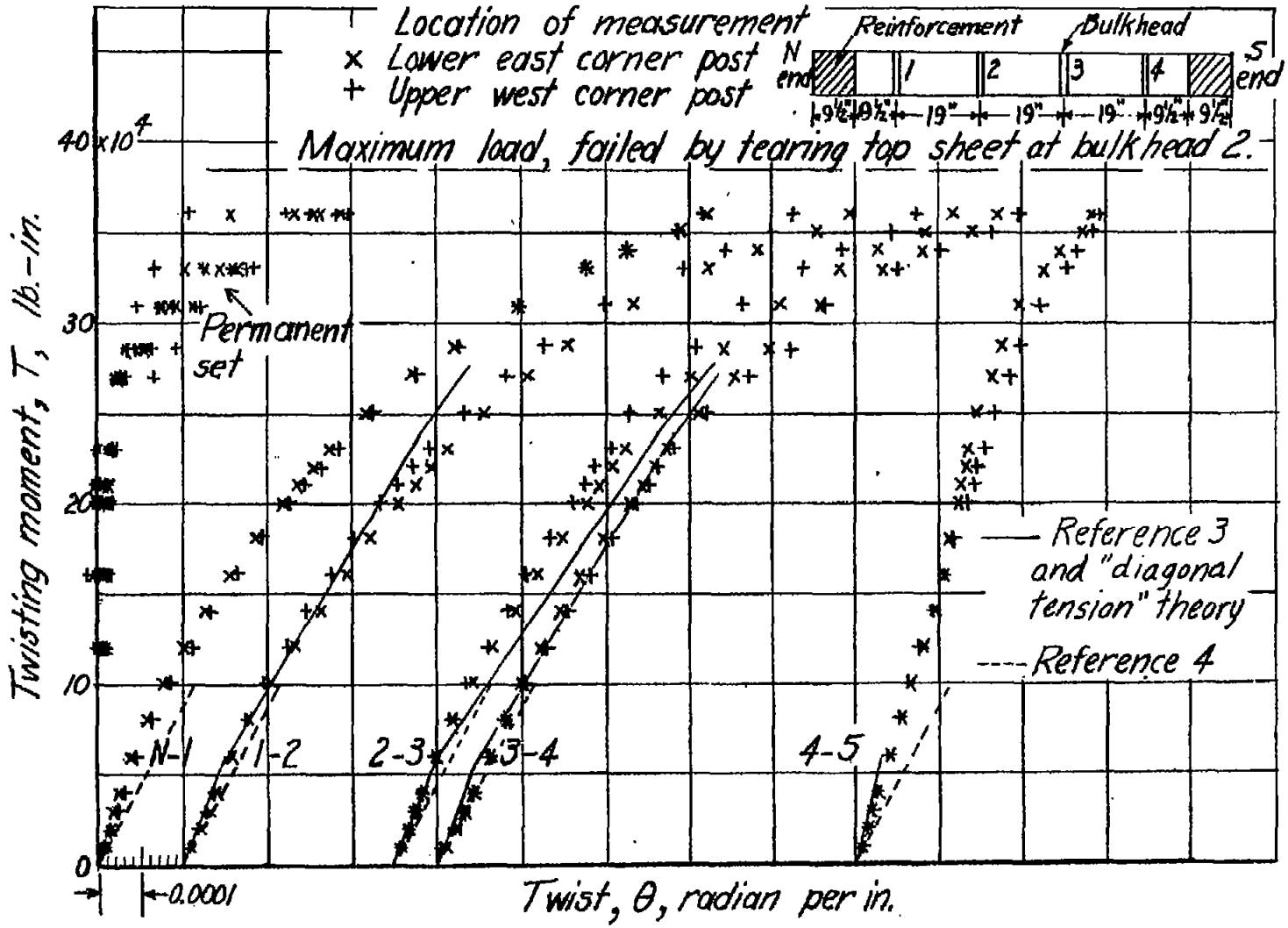

Figure 7.- Average twist between bulkheads.

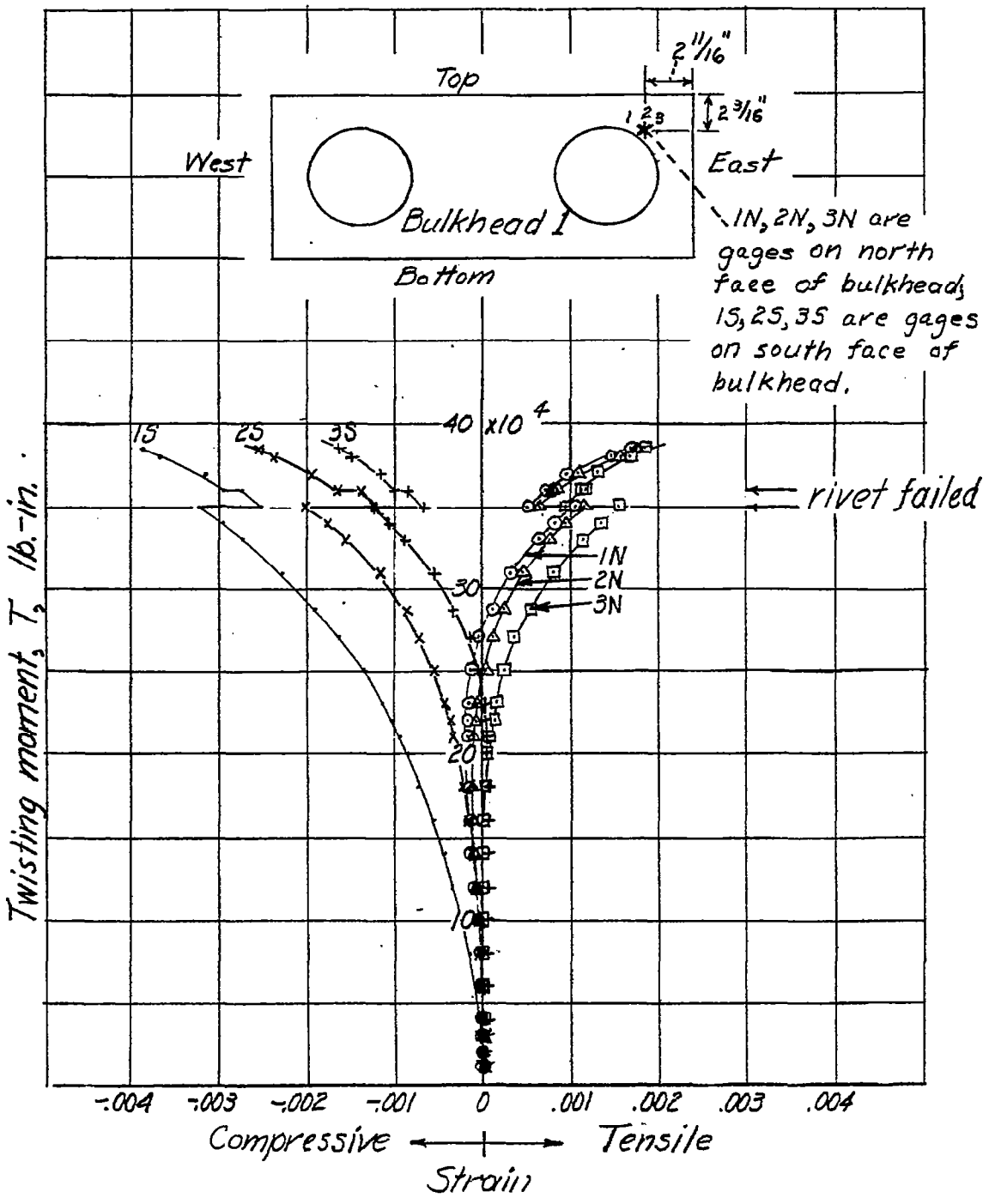

Figure 8.- Extreme fiber strain in corner of bulkhead 1.

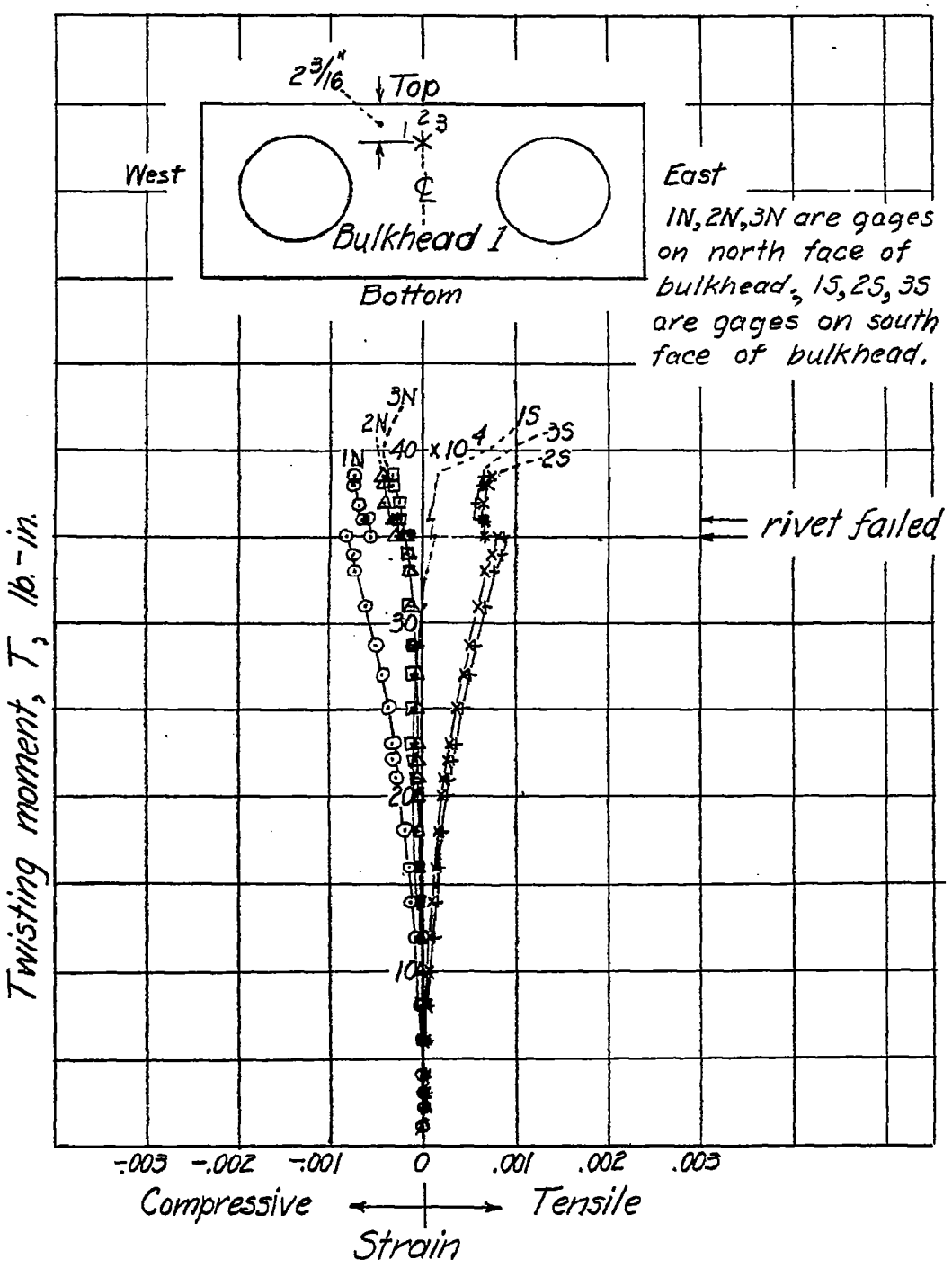

Figure 9.- Extreme fiber strain at top center of bulkhead 1.

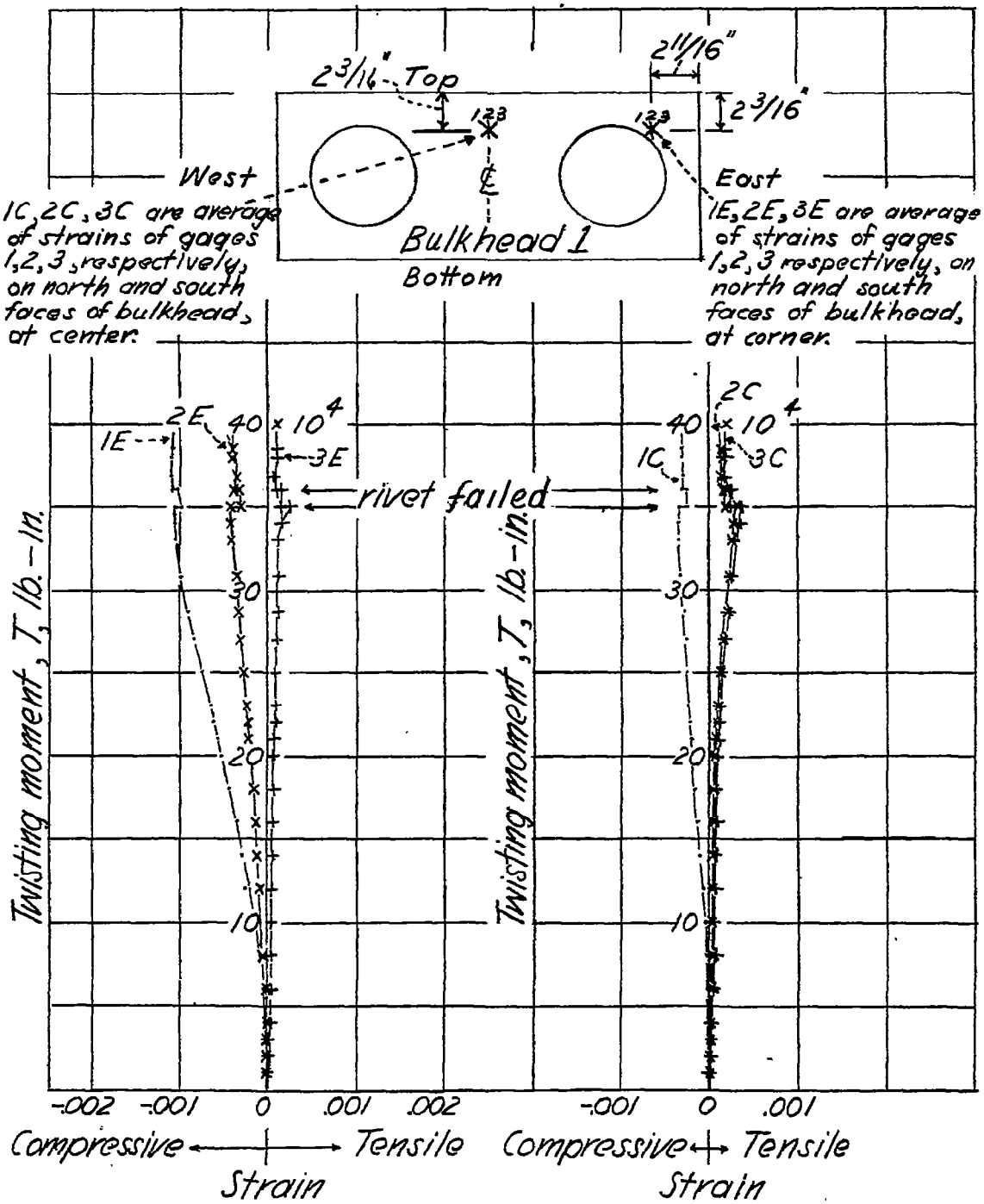

Figure 10.- Median fiber strain in bulkhead 1.

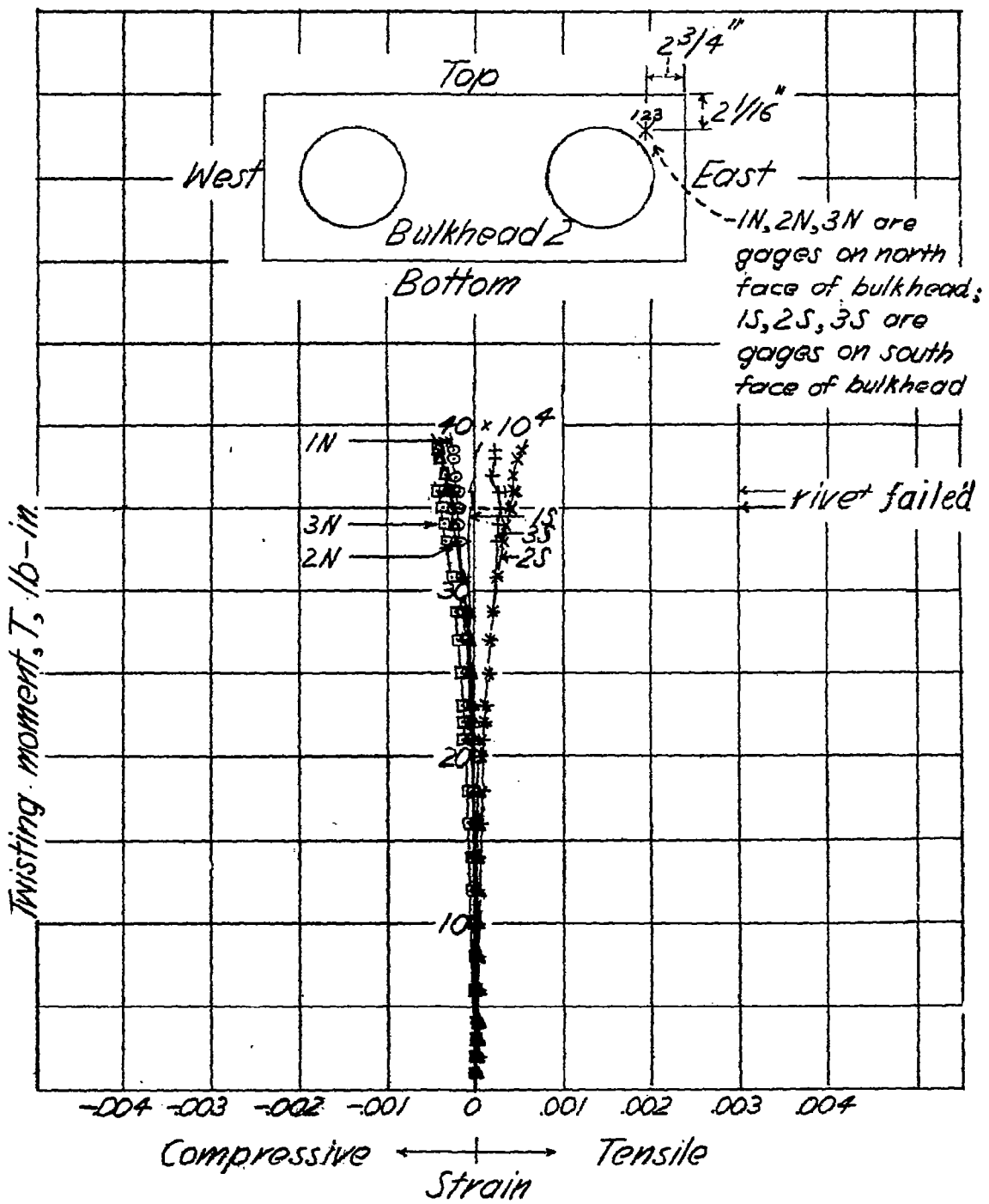

Figure 11.- Extreme fiber strain in corner of bulkhead 2.

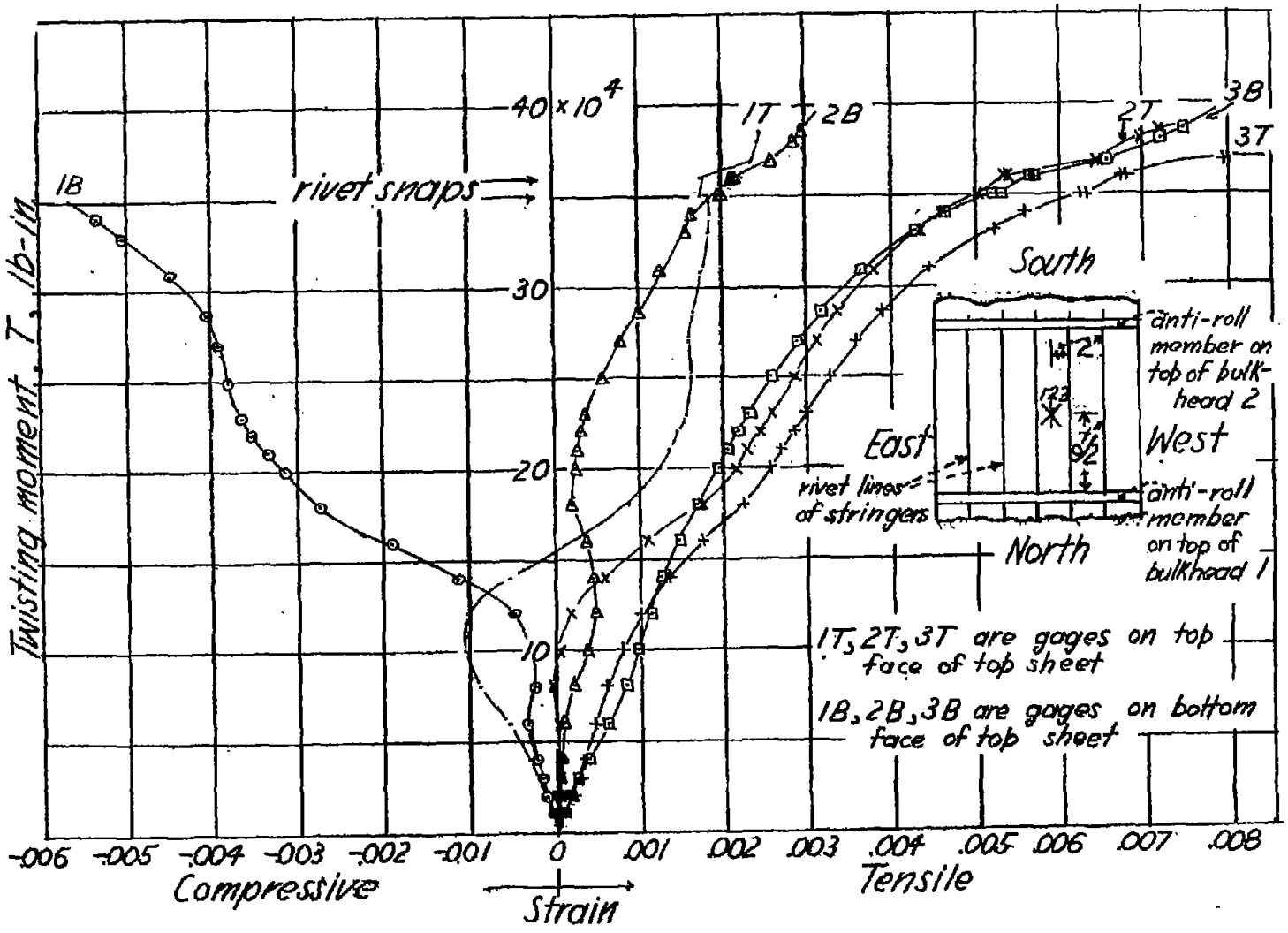

Figure 12.- Strains at center of top sheet between bulkheads 1 and 2 and between stringers 3 and 4 (counting from east corner).

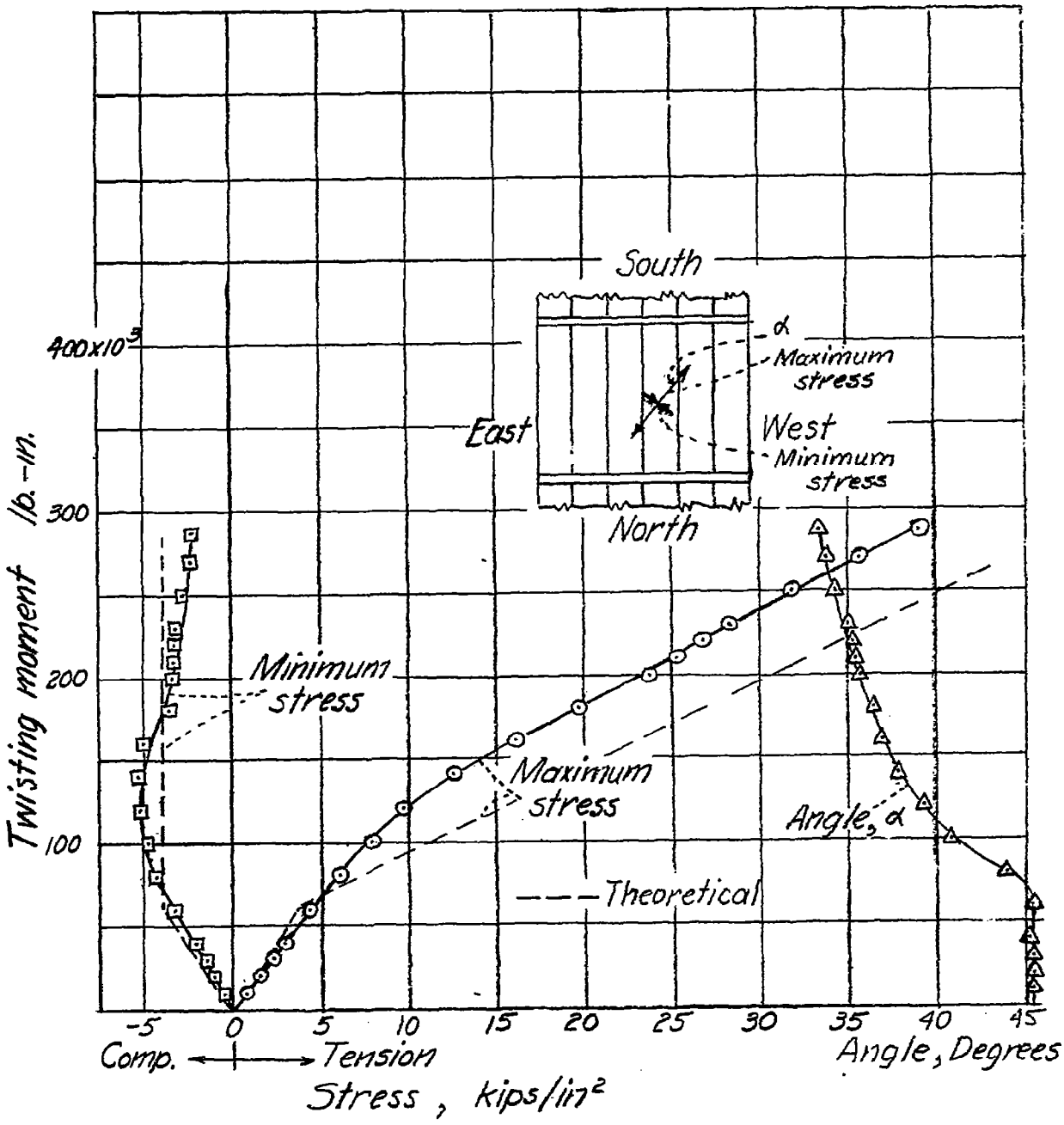

Figure 13.- Maximum and minimum principal stresses at the median plane of the top cover sheet between bulkheads 1 and 2.

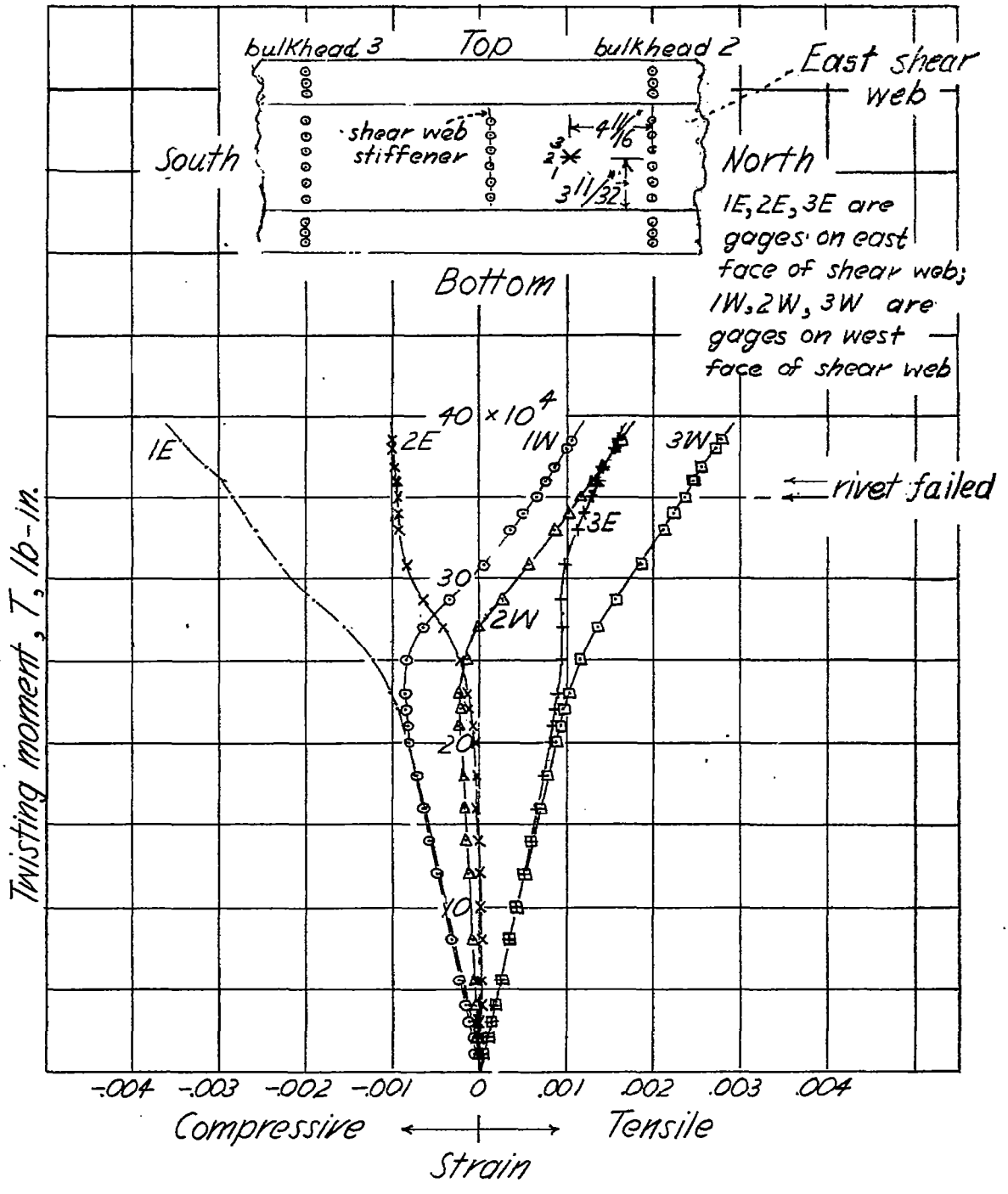

Figure 14.- Strains at center of east shear web between bulkhead 2 and shear web stiffener.

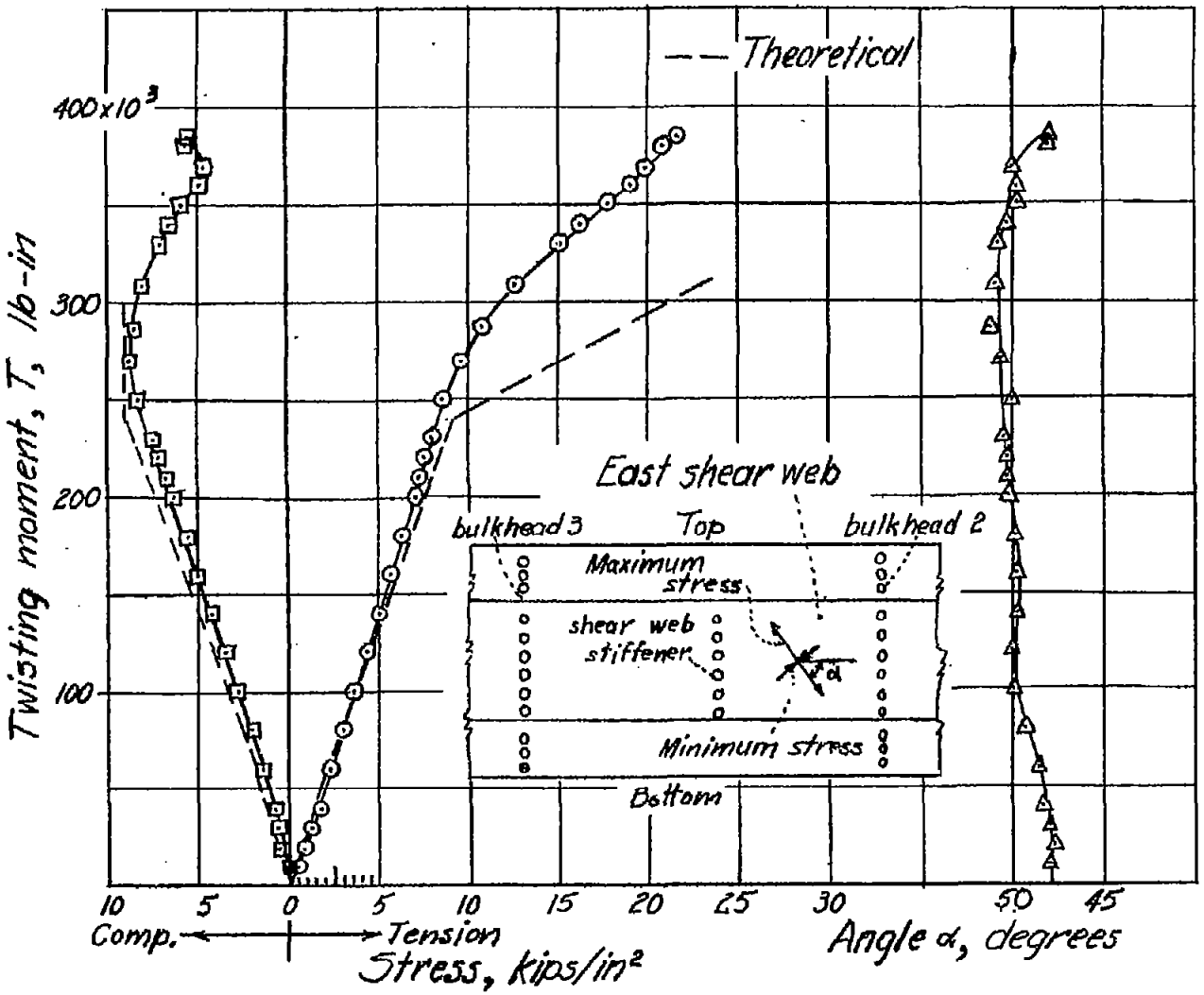

Figure 15.- Maximum and minimum principal stresses at the median plane of the east shear web between bulkheads 2 and 3.

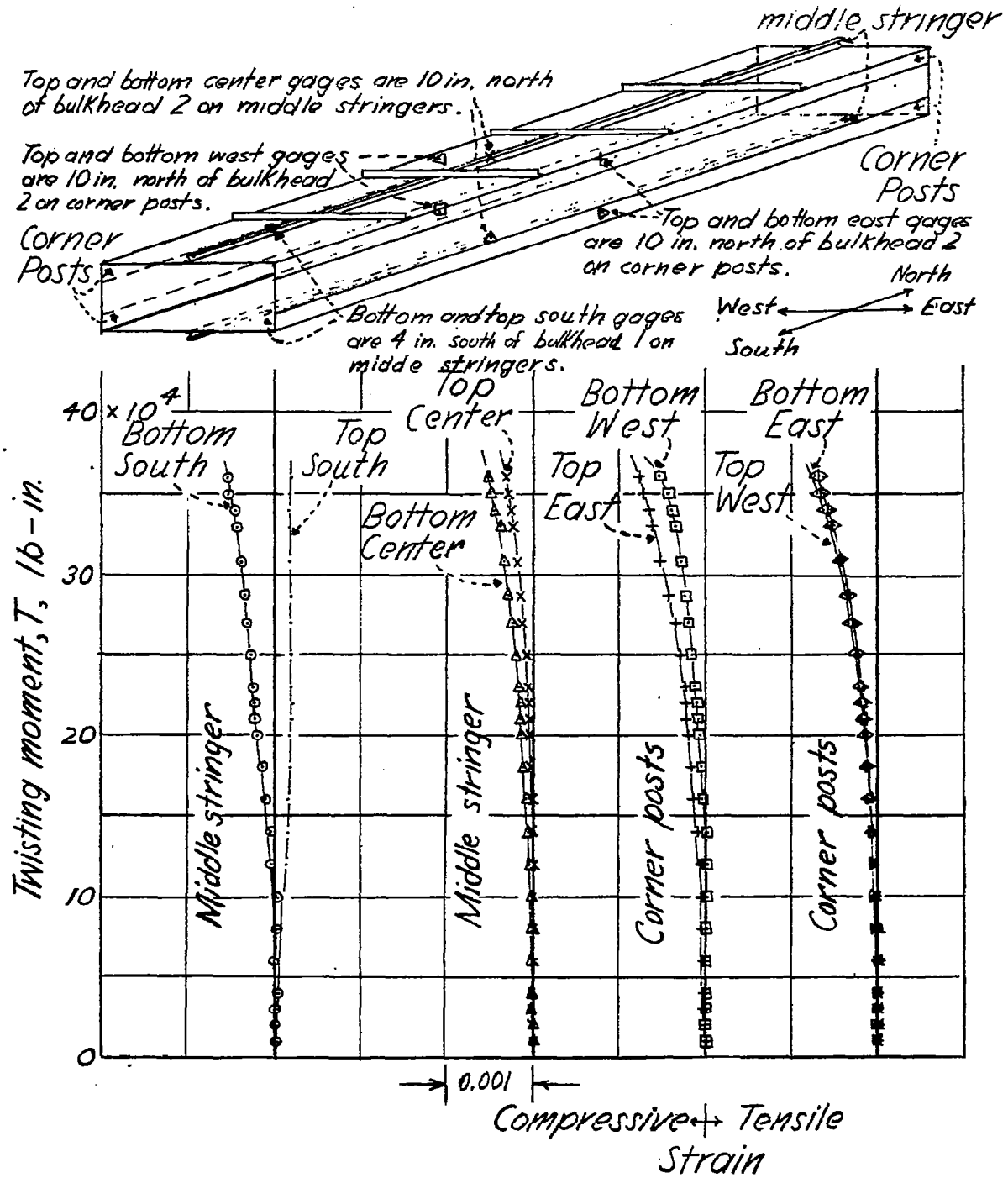

Figure 16.- Strains at points 4 in south of bulkhead 1 and 10 in north of bulkhead 2 on top and bottom middle stringers and at points 10 in north of bulkhead 2 on all four corner posts.

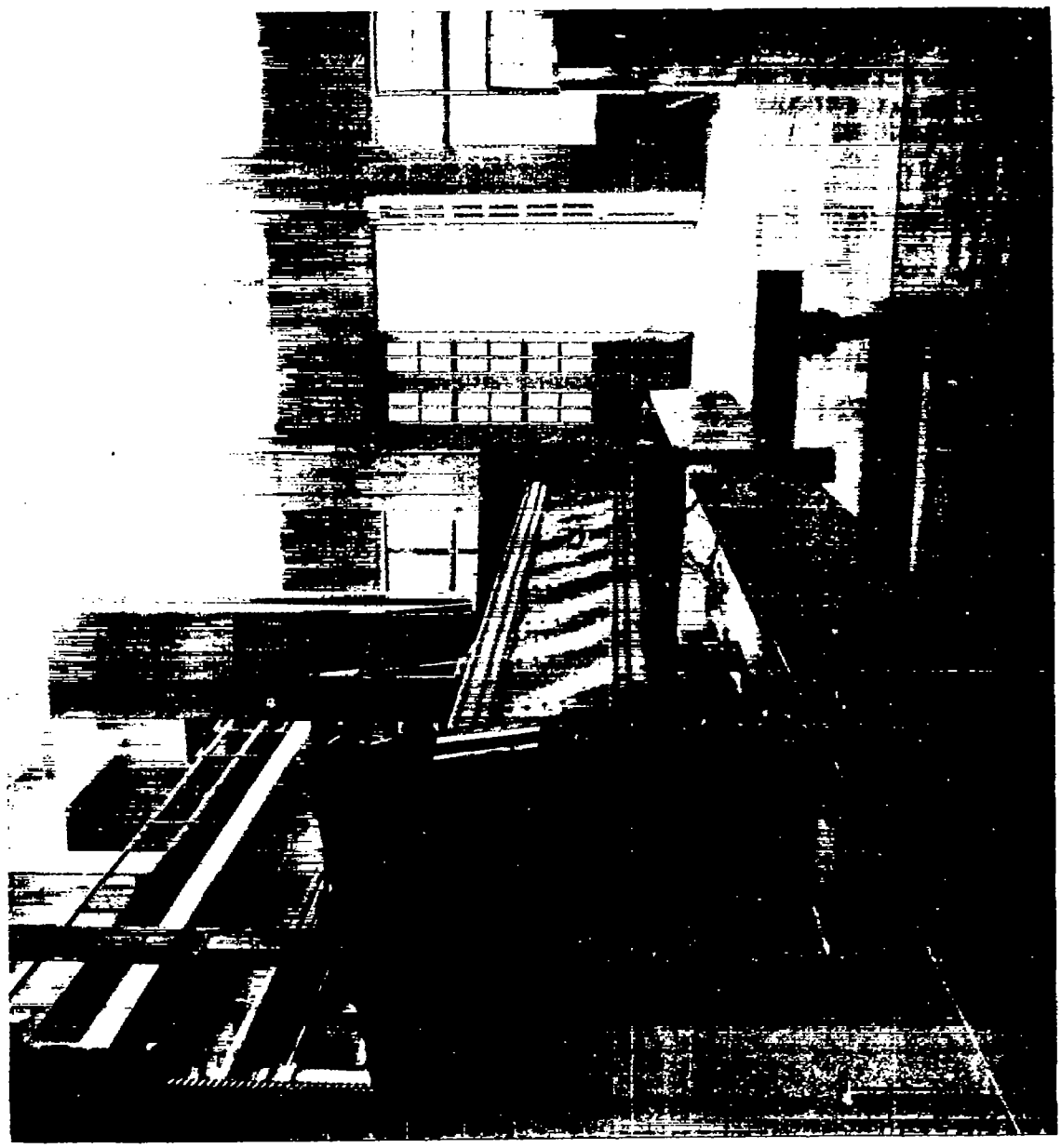

Figure 17.- Buckles in the east shear web of the monocoque box at failure.

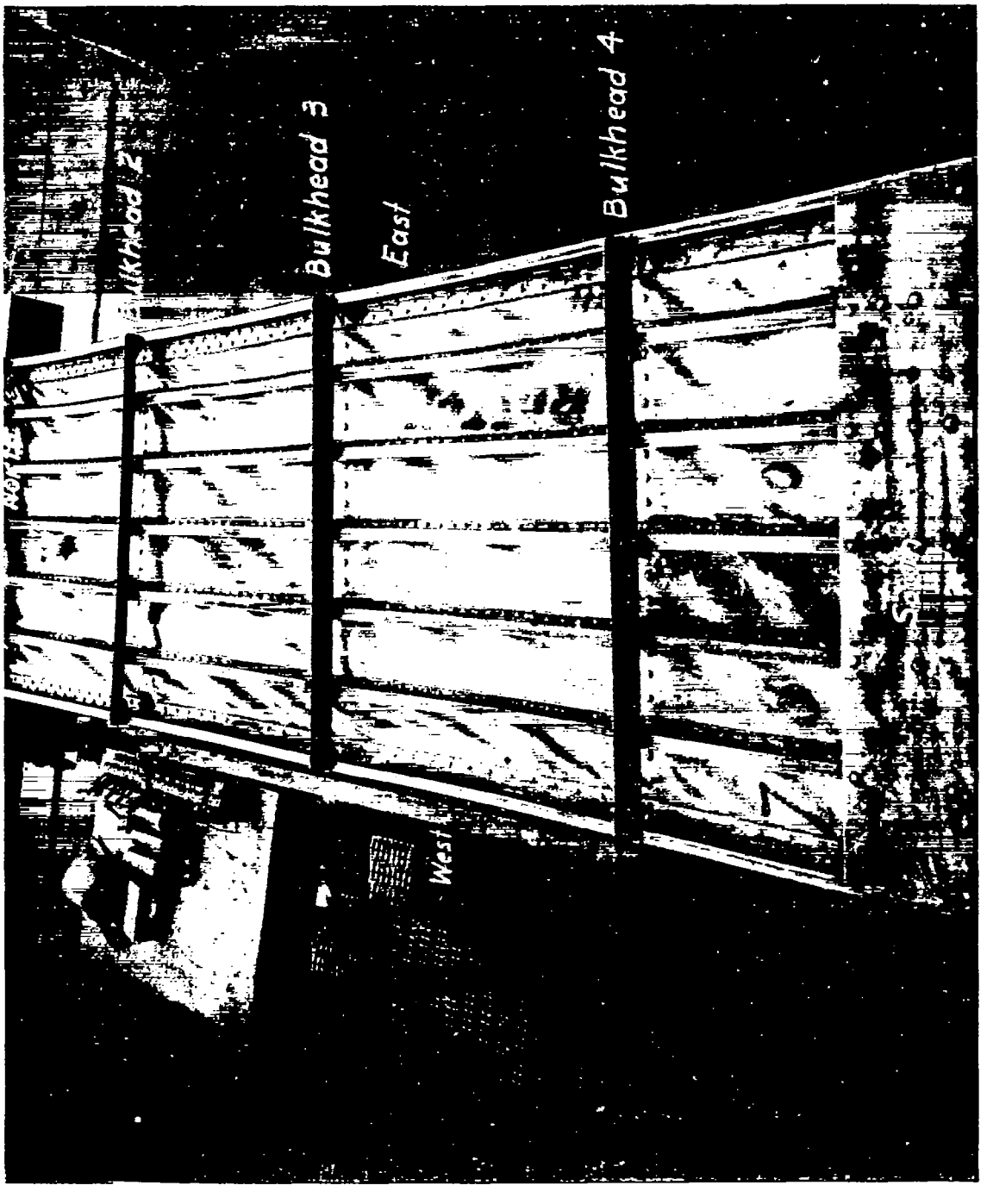

Figure 18.- Buckles in top cover sheet at failure.

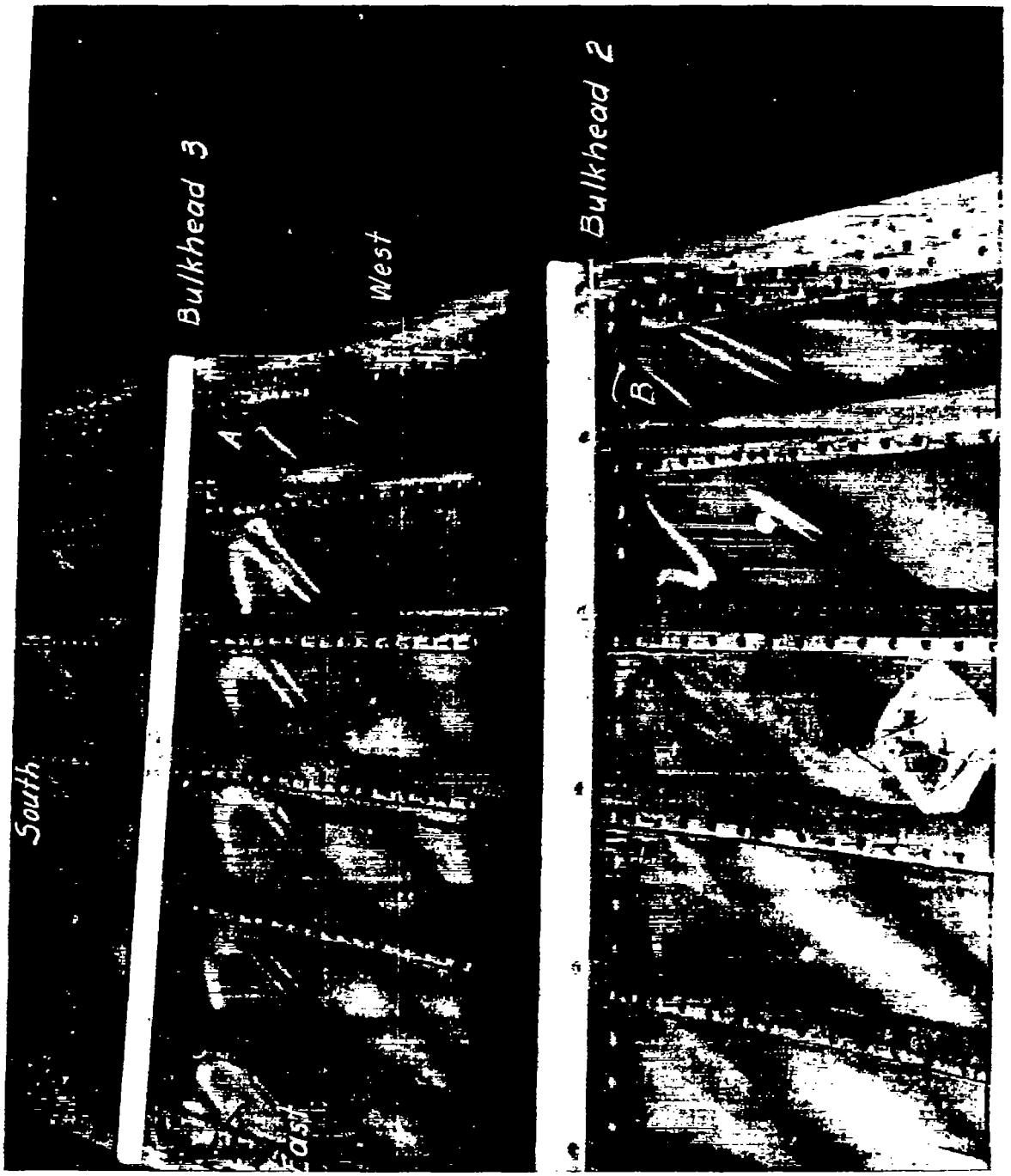

Figure 19.- Failure of a rivet at A on bulkhead three and tearing of the top cover sheet at B on bulkhead two.

Figure 20.- Failure of rivets joining antiroll to corner post.

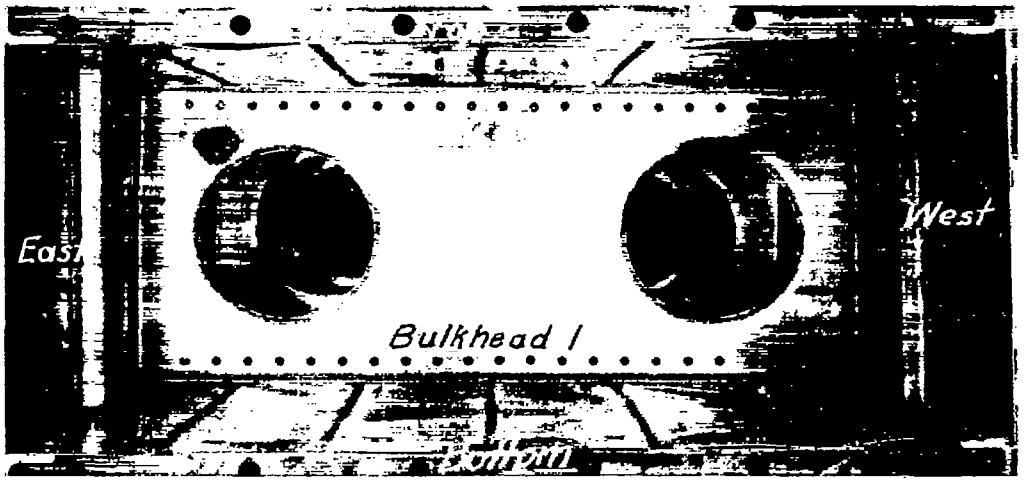

Figure 21.- Bulkhead one after failure.

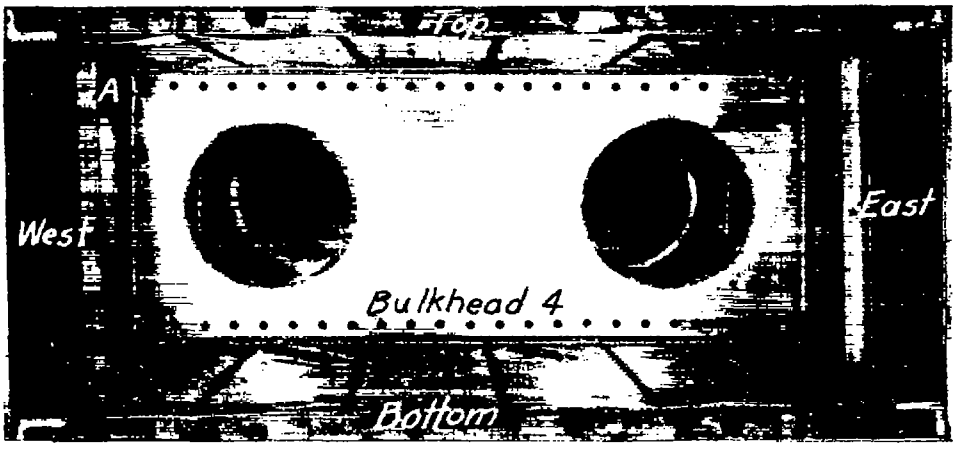

Figure 22.- Bulkhead four after failure showing permanent buckle near A.

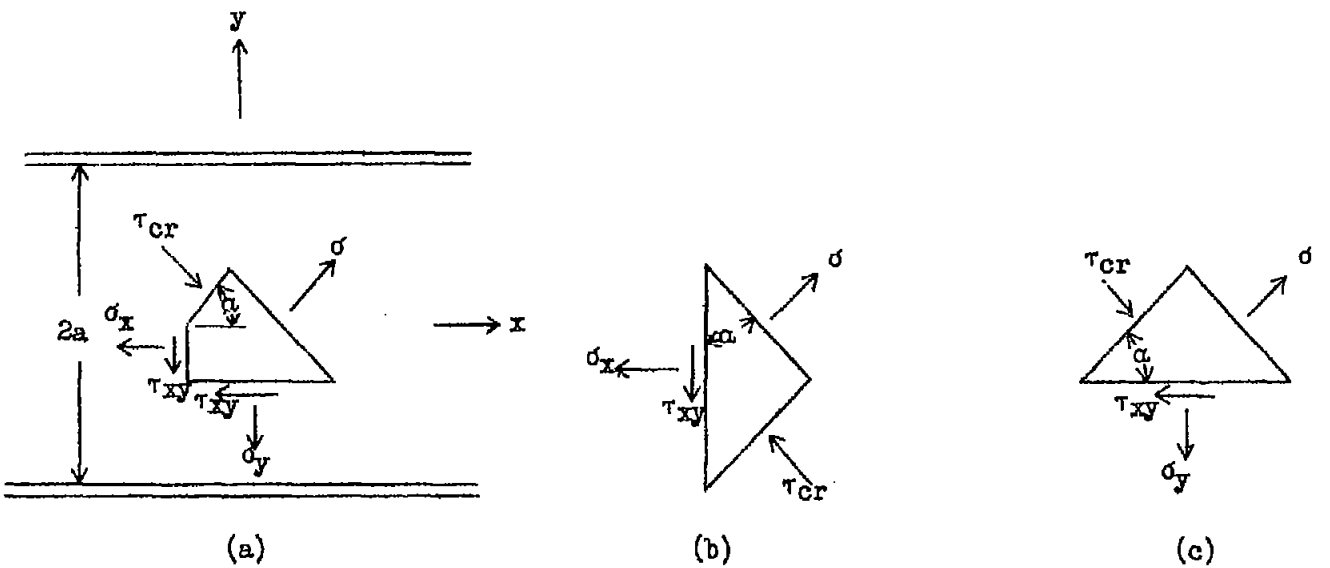

Figure 23.- Stresses at the midthickness for "diagonal tension".